Department of Chemical Engineering

Thermal-Generated Surfactant Flow at the Air/Water Interface: Experimental Observation and Theoretical Modelling

Trung Bao Nguyen

This thesis is presented for the Degree of
Doctor of Philosophy
of
Curtin University

May 2018

DECLARATION

To the best of my knowledge and belief this Thesis contains no material previously published by any other person except where due acknowledgment has been made.

This Thesis contains no material which has been accepted for the award of any other degree or diploma in any university.

Signature: …….

Date: **04/05/2018**……

ACKNOWLEDGEMENT

First, I would like to thank my supervisor, Dr. Chi Minh Phan for his support during my Ph.D. journey. Without him, this thesis could not be built and completed successfully. His supervision and contribution are not only critical but also encouraging. I would also like to thank my co-supervisor, Dr. Gia Hung Pham for his guidance and advice to my study.

I acknowledge Curtin University and Department of Chemical Engineering for supporting me not only a scholarship but also three unforgettable years in Perth.

My warm thanks are also given to staffs of Chemical engineering Laboratory. I appreciated their kind supports during my study.

My big thank is for Dr. Doan Nguyen, Mrs Trang Le, Dr. Cuong Nguyen and Mr. Cuong Cao who helped me to settle down in Perth. I specially thank to my Curtin soccer team (Dr. Tin Do, Mr. Khai Tran, Mr. Khanh Nguyen, Dr. Long Nguyen, Dr. Viet Nguyen, Dr. Hoang Nguyen, Dr. Thong Kieu, Dr. Quan Tran, Dr. Thanh Do, Mr. Nghia Nguyen…) for the unforgettable moments that we have been through. I am also deeply grateful to Dr. Ha Bui, Mr. Trong Luu and Mr. Youi Vo for many relaxed dinners.

Last but not least, I would like to thank my family for their unconditional love and support. I am indebted my parent (Mr. Hoa Nguyen and Mrs. Van Bien) who had sacrificed most of their life raising and encouraging me to pursue the academic career.

ABSTRACT

Surfactants have been widely utilized for many industrial applications as their ability can reduce the surface tension during the adsorption process. It should be noted that surfactants (in their water solutions) are very sensitive to thermal effect. In general, the temperature change can generate a surface tension gradient and Marangoni effect. However, such Marangoni effect-based thermal-generated surfactant flow has not been quantified carefully so far.

This Thesis focused on both experimental and theoretical developments of such phenomena. Firstly, experiments were performed to observe the phenomena. Secondly, theoretical models were developed to quantify and verify the phenomena. Furthermore, the influence of surfactant structures was also evaluated by changing different surfactants.

The phenomenon was first discovered by observing the motion of a floating Teflon ball at the air/water interface under thermal effect in presence of Triton X-100. It is interesting that such motion could not be observed by using pure water, CTAB or SDS. A Teflon-coated Tungsten wire was used as a source of the thermal effect. The wire was intended to put above the interface to eliminate the bulk flow impact. The phenomena were then quantified by developing two theoretical models. These models were finally verified to select the appropriate mechanism.

In this thesis, the change of surface tension of Triton series under temperature effect has been experimentally measured with and without NaCl. The linear relationship has been confirmed and consistent with the literature. These data were then used to study the influence of hydrophilicity of Triton series on the phenomena. It has been found

that increasing hydrophilicity generated to the faster motion but stopped at the shortest distance.

In summary, this is the first time the thermal-generated surfactant flow has been experimentally quantified. The theoretical development was then carried out to quantify and verify the phenomena. Additionally, the phenomena can be controlled by varying the hydrophilicity of surfactants. The phenomena open up an avenue to control the surfactant flow in microfluidic applications.

PRODUCED DURING THIS PHD STUDY

JOURNAL ARTICLES

Published:

1. **Nguyen, T.B.** and C.M. Phan, *Surface flow of surfactant layer on air/water interface.* Colloids and Surfaces A: Physicochemical and Engineering Aspects, **2017**. 530 (Supplement C): p. 72-75
2. **Nguyen, T.B.** and C.M. Phan, *Influence of surfactant hydrophilicity on the thermal-driven air/water surface flow.* ACS Omega, **2018**. 3 (8), 9060-9065
3. **Nguyen, T.B.** and C.M. Phan, *Influence of temperature on the surface tension of Triton surfactant solutions.* The Journal of Surfactants and Detergents, **2018.** ***Accepted*** *(*10.1002/jsde.12228).

Table of Contents

List of figures

List of Tables

LIST OF ABBREVIATIONS

BM	Benard-Marangoni
CMC	Critical micelle concentration
CTAB	Cetyltrimethylammonium bromide
EO	Ethylene oxide
SDS	Sodium dodecyl sulfate

LIST OF SYMBOLS

Chapter 1 Introduction

1.1. Background

Surfactants are widely used in many applications such as foamability, wettability, coating, flotation, mineral and coal extraction and so on. In general, they consist of two parts in their molecular structure: head and tail. While the head is hydrophilic, tail on the other hand is hydrophobic. When surfactants are dissolved in water, they adsorb into the interface. Basically, this process reduces the surface tension of the solution. The adsorption of surfactants has been researched for several decades due to their greatly-practical applications.

Marangoni effect was first discovered by observing the tear of wine. In general, the liquid in the region with low surface tension tends to move to the high surface tension area. The gradient of surface tension can be caused by the different concentration or temperature. This phenomenon is the basic underlying mechanism for many applications such as microfluidics, actuators etc…

The motion of the flow or an object in different phases is greatly obtained attention from the scientists as it is one of the core factors in many applications such as microfluidics. So far, there is a huge number of researches has been done to satisfy not only the curiosities but also the practical aims. The scientist can use various ways to induce such movement such as electricity, chemicals, light sources, thermal and so on [1-5]. One of the drawbacks in this area would be the quantification of the movement as it remains unclear.

1.2. Objectives of this thesis

Although a lot of researches have been carried out so far, there is no observation of surface flow which was induced by thermal sources. In this thesis, the main objectives are to introduce new phenomenon related to the motion of surface flow and quantification:

- Investigating the effect of temperature on the surface tension of surfactant solution. This will help to understand insights into the mechanism of surface flow under thermal effect.
- The novel phenomenon so-called surface flow has been discovered by observing the movement of an alternative object on the surface of surfactant. The theoretical models are developed and verified.
- The work has been further studied with a series of surfactants with the difference of structure to investigate the impact of hydrophilicity on such movement.

1.3. Format of the thesis

Chapter 1. This chapter firstly discusses general information of surfactant and the adsorption of surfactants. Secondly, it describes one of the most famous phenomena so-called Marangoni effect. Finally, a brief introduction of object or flow motion is represented.

Chapter 2. This chapter details on surfactant and the adsorption of surfactant. A basic knowledge of Marangoni effect is also included. In addition, the theory and review of the thermal-induced movement have been done to highlight the significance of this study.

Chapter 3. Chemicals were used straight away without any further purification in this study. This chapter also listed the methods for measuring equilibrium and dynamic surface tension. The brief description of the method used to carry out experiments was also included.

Chapter 4. Illustrating detail experimental procedure to measure either equilibrium surface tension or dynamic surface tension under thermal effect. The results were then used for the next chapters.

Chapter 5. Surface flow experiment was introduced by employing floating Teflon ball. This chapter also described the insight of the phenomenon with detailed quantification.

Chapter 6. Further studies on the different structure of Triton series surfactants were performed to understand the hydrophilic impact on such flow.

Chapter 7. Conclusion and future recommendations.

Chapter 2 Literature review

2.1. Surfactants, interfacial phenomena and adsorption of surfactant.

The definition of a surfactant is considered as a material that can make a huge reduction in the surface tension (γ) of water when low concentrations are used. In general, there are two parts of surfactant molecules which are hydrophilic (head) and hydrophobic (tail). The head was proved to be easily dissolved in water than in oil or air [6]. As a result, surfactants can provide important interfacial properties for applications. For instance, a surfactant can decrease the surface tension in aqueous solution. In addition, general surfactant molecules will be self-assemble so-called micelles after reach the critical micelles concentration (CMC)

2.1.1. Interfacial phenomena

The surfactant's properties at the interface are the key factors for many applications such as foam stability, coating flows, foamability, wettability, the formation of soap-lather [7]. It is claimed that not only equilibrium but also dynamic behaviour is significant in fast processes. For example, in the cosmetic industry, surfactants are initially utilized as cleansers, wetting agents, foaming agents. Later on, their applications on different dispersed systems are also widely applied such as personal care products [8]. In addition to this, in order to enhance oil recovery, surfactants are also applied to decrease the surface tension and other properties with the purposes of recovering a bigger amount of oil from a water-pumped reservoir [9].

2.1.2. Surfactant and applications

The structure of surfactant molecule is basically created by two main parts, tail and head. The hydrophobic tail contains any type of linear, branched or aromatic hydrocarbon chain. Some of them even possess more than one hydrophobic groups [10]. Figure 2.1 shows the common surfactant classification based on the polar head.

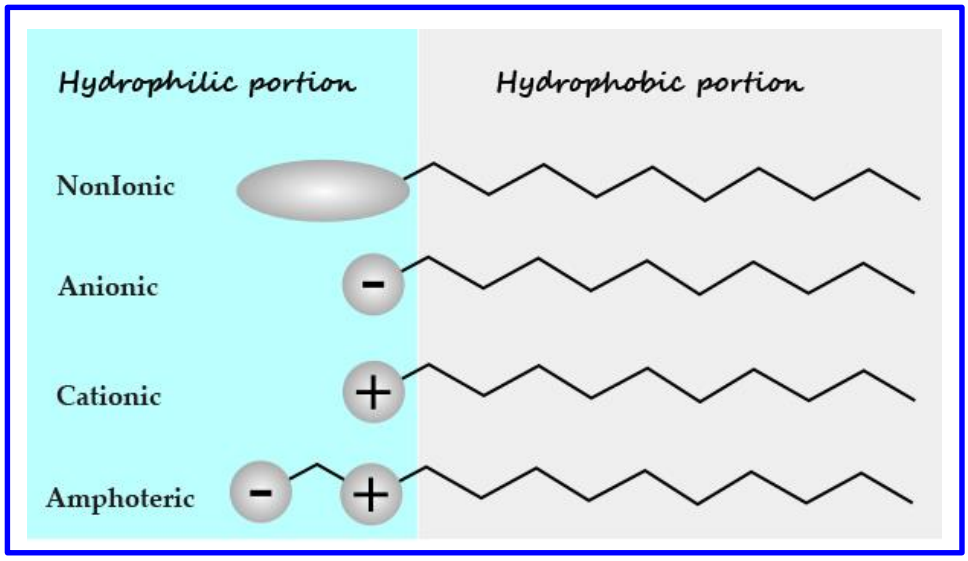

Figure 2.1. The different types of surfactants.

Nonionic: There is no apparent ionic charge in this surfactant because of the non-dissociable hydrophilic group. The wide range of this surfactant can be listed as ester, ether, long-chain alcohol, amide [11]. At high concentration, these can be used as resistant substances against hard water, polyvalent metallic cations, and electrolyte. Additionally, these types of surfactant are great detergents in term of eliminating oily soil and often present in laundry products. Furthermore, they are also applied in other applications such as cosmetic emulsifiers, food emulsifiers.

In industry, nonionic surfactants contribute approximately 45% in total and become the second biggest use [12]. In the past, some low poisonous surfactants with the glucoside head group were brought into the market but for now, polyethylene oxide

and polypropylene oxide with the lipophilic group has dominated by the boom of oil and gas industry with much cheaper production.

Anionic: The head of these surfactants consist of anionic functional groups such as sulphonate, sulfate, phosphate. Generally, an alkaline metal (Na^+, K^+, NH_4^+) is the counterions. The contribution of these surfactants is around 50% in total [12]. There are some of the straight-chain acid based sodium and potassium salts adding to stop precipitation of alkylbenzene sulfonates, lauryl sulfate. The anionic surfactants contributes 50% of industrial production.

Cationic: The positive charge is located at the head of surfactants such as R-N(CH3)3+Cl-, RNH3+Cl-. When these surfactants are dissolved in water, they will be split into two parts, an amphiphilic cation and an anion. The main drawback of cationic surfactants is the expensive synthesis that preventing them to be widely used. As a result, they are normally utilized in some specific cases such as a bactericide or a corrosion inhibition [13].

Amphoteric: This type of surfactants possess both cationic and anionic heads attached to the molecular structure. Benefiting from the special properties, the adsorption can be occurred either on positive or negative charge surface [14]. Nevertheless, most organic solvents cannot dissolve these surfactants [15]. They are generally mild, and are widely applied in pharmaceutical fields as personal care products such as shampoos, body wash, and shaving products.

2.1.3. Adsorption of surfactants at the air/water interface

The process of transferring surfactant molecules from bulk to interface of the surfactant solution is called adsorption of surfactant [14]. The migration of surfactant molecules onto interface will decrease the surface tension. If the surface tension is changed with time, it will be called dynamic surface tension. The saturation of surfactant concentration is reached after a period of time and the surface tension stops changing with the value defined as equilibrium surface tension.

Surfactants have a tendency to set up the interfacial conditions via highly surface active region which is adsorbed at the interface. These adsorption phenomena have been studied deeply in the couple decades [6-22] with the purposes of solving the below questions:

- Surfactant concentration at the interface.
- Surfactant packing and orientation at the interface.
- Adsorption rate.
- The energy changes in the system, such as ΔG (free energy), ΔS (entropy), or ΔH (enthalpy)

There are different approaches that can be used to measure the surfactant adsorption and the adsorption layer structure such as surface tension and surface potential.

2.1.3.1. Surface tension

The use of this method to represents the adsorption at the air/water interface is not only simple but also effective. A mathematical model is used to fit the experimental data and produce the adsorption parameters. These parameters will reveal the surfactant's efficiency and effectiveness. There are two kinds of surface tension measurement: equilibrium and dynamic.

Equilibrium surface tension

This is one of the most well-known factors to investigate the surfactant adsorption. At room temperature (25^{o}C), the value of equilibrium surface tension is at around 72 mN/m for pure water [23, 24]. In contrast with the lower value of surface tension when adding surfactants, the presence of salts normally increase the surface tension. There are some popular methods using to measure the equilibrium surface tension such as Wilhelmy plate method, Du Nouy ring method or drop volume method [25]. The fit of experimental data into a model is used to describe the equilibrium surface activity. The Gibbs equation can be employed to obtain the surface excess or surface concentration of surfactant.

$$\Gamma = -\frac{1}{nRT}\frac{d\gamma}{d\ln(c)} \qquad (2\text{-}1)$$

where Γ is equilibrium surface excess, n = 1 for non-ionic surfactants, neutral molecules or ionic surfactants in the presence of the excess electrolyte, and n = 2 for 1:1 ionic surfactants. R is the gas constant, T is Kelvin temperature, c is the bulk surfactant concentration.

There are other isotherms which can be used as well such as Henry isotherm. Langmuir isotherm, Frumkin isotherm.

Henry isotherm

$$\Gamma = K_H c$$

where K_H is the equilibrium adsorption constant

Langmuir isotherm$\Gamma = \Gamma_m\left(\frac{Kc}{1+Kc}\right)$

$$\Gamma = \Gamma_m\left(\frac{Kc}{1+Kc}\right)$$

where Γm is maximum surface excess, K is Langmuir equilibrium adsorption constant.

Frumkin isotherm

$$\pi = -\mathrm{nRT}\Gamma_m ln\left(1 - \frac{\Gamma}{\Gamma_m}\right) - \frac{nRTA}{2}\Gamma_m\left(\frac{\Gamma}{\Gamma_m}\right)^2$$

where A is the constant which depends on the non ideality of the layer.

Dynamic surface tension

This value manipulates a great number of core biological and industrial processes [6-17, 26].

It is proved that the surfactant adsorption is time-dependent. The surfactant reduces the surface tension from solvent value to equilibrium value during the adsorption. Depending on the concentration and the surfactant nature, this process varies from milliseconds to days. Many methods can be applied to measure this value such as force methods, shapes methods and pressure methods.

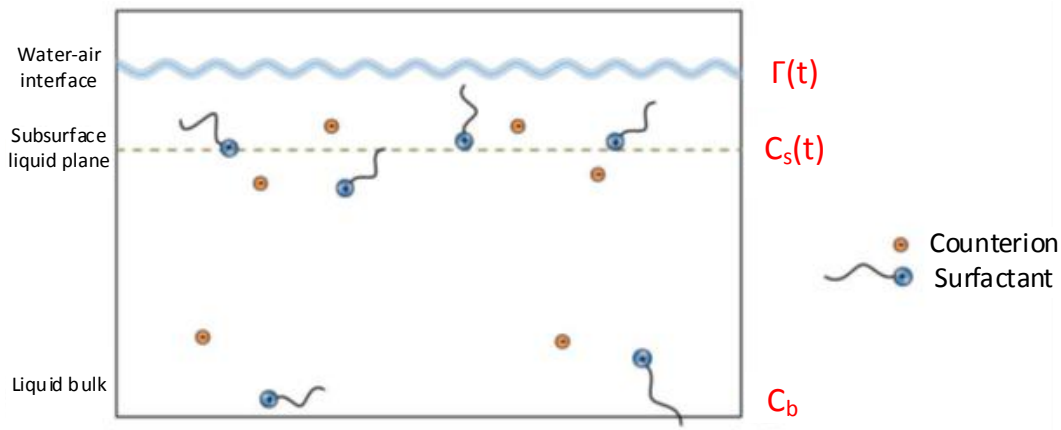

Figure 2.2. Dynamic adsorption of cationic surfactants at the air/water interface [27].

As can be seen from Figure 2.2 that from the bulk, the diffusion of surfactant molecules is initially done in the sub-surface layer.

The adsorption of these molecules is then occurred at the interface prior any molecular arrangement [7]. There are various proposed models in literature has been produced to investigate this dynamic adsorption process.

Diffusion-controlled: This model assumes that the diffusion of monomers is adsorbed immediately at the interface. In other words, the adsorption process is rapid and the diffusion process is the step of controlling rate.

The mixed kinetic-diffusion: The diffusion of monomers is assumed to create the bulk of the sub-surface. Nevertheless, the rate-controlling step dominates the migration of these monomers to the interface. As a result, it can be stated that there is an adsorption barrier to prevent monomers transferring to the interface [28].

2.1.3.2. Surface potential of air/water interface

The distribution of electrical charges is not always equal amongst phases at any interface. Different net charges of different signs are then created on both sides. Consequently, they make a raise of potential across the interface and are called electrical double layer [26]. The different potential is noted by the surface potential at the air/liquid interface [29].

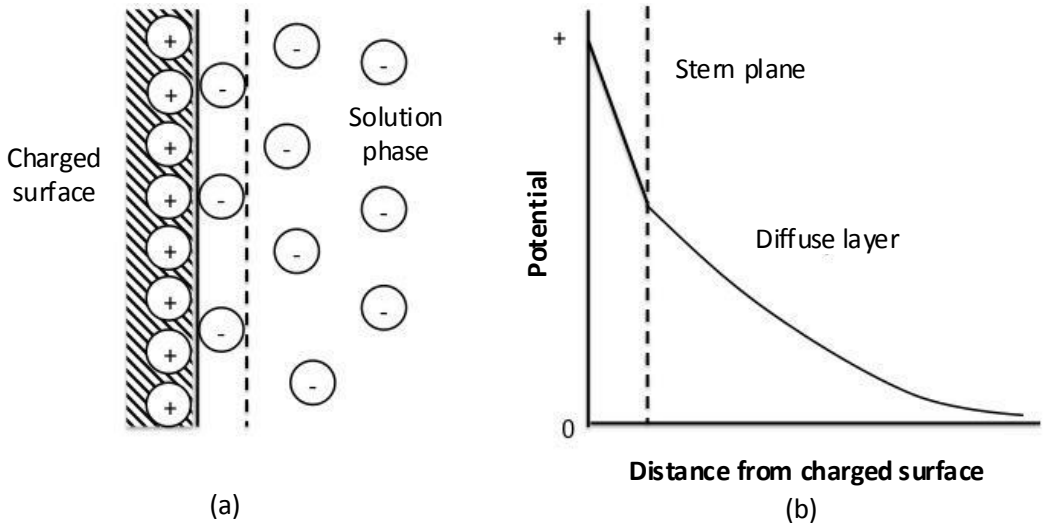

Figure 2.3. Stern model: (a) Counter-ions distribute to the vicinity of the charged surface; (b) Electrical potential is changed with distance.

As can be seen in Figure 2.3, the electrical potential declines shapely in the Stern layer and gradually in diffuse layer. The charged surface can be even changed the sign due to the counter-ions of the Stern layer.

In conclusion, the combination of surface potential and surface tension can supply reliable insights of molecular structure at the interface. Surface potential is an even better method in some cases than surface tension [30]. There are some experimental methods which can be used to measure the surface potential such dynamic capacitor, radioactive probe and jet electrode [31].

2.1.3.3. Influence of salts on the surface tension of surfactant solutions

As discussed above, the adsorption of surfactant drives by hydrophilicity, which can be affected by electrolytes. In general case, adding salts, such as NaCl, will increase the adsorption at air/water interface. In literature, there is no report related to the effect of NaCl on the surface tension of Triton solutions with and without varying temperature.

2.1.4. Adsorption of surfactants at the solid/water interface

The surfactant adsorption phenomena at the solid/liquid interface is a key role in various applications, such as mineral flotation, detergency, dispersion of solids, corrosion inhibition, oil recovery [32-36]. There are various factors that can highly impact on the adsorption of surfactants at the solid/liquid interface:

- The molecular nature of surfactant (hydrophilicity, hydrophobicity).
- The structural nature of interfacial groups on the solid surface (non-polar sites, highly charged sites).
- The aqueous phase (pH, electrolyte, other additives).

Mechanism of adsorption

The basic underlying mechanisms are described intensively in the literature [10]. Single ions rather than micelles are involved in the adsorption of surfactant [37]. These mechanisms are listed below:

- Ion exchange: The charged ions of surfactant replace the adsorbed counter ions onto the substrate.
- Ion pairing: This process describes how surfactant ions will be adsorbed onto oppositely-unoccupied charged sites by counterions.
- Hydrophobic bonding: When an adsorbed molecule with hydrophobic group attracts a solution-present molecule.
- Adsorption by the polarization of π electrons: This mechanism occurs when strongly-positive sites of solid adsorbent meet the surfactant with the rich π electron.

Adsorption isotherm

The charged solid surfaces in the aqueous phase are either negative or positive. These charger surfaces are generated by the dissociation/ionisation of surface groups or solution ions adsorbed to the uncharged surface. Hence, at the solid/liquid interface, it can be stated that the electrical double layer is normally key factor for the adsorption. There are different types of surfactants and leads to various research on adsorption of these surfactants at the solid/liquid interface. In this thesis, all of the experiments are prepared by using non-ionic surfactants.

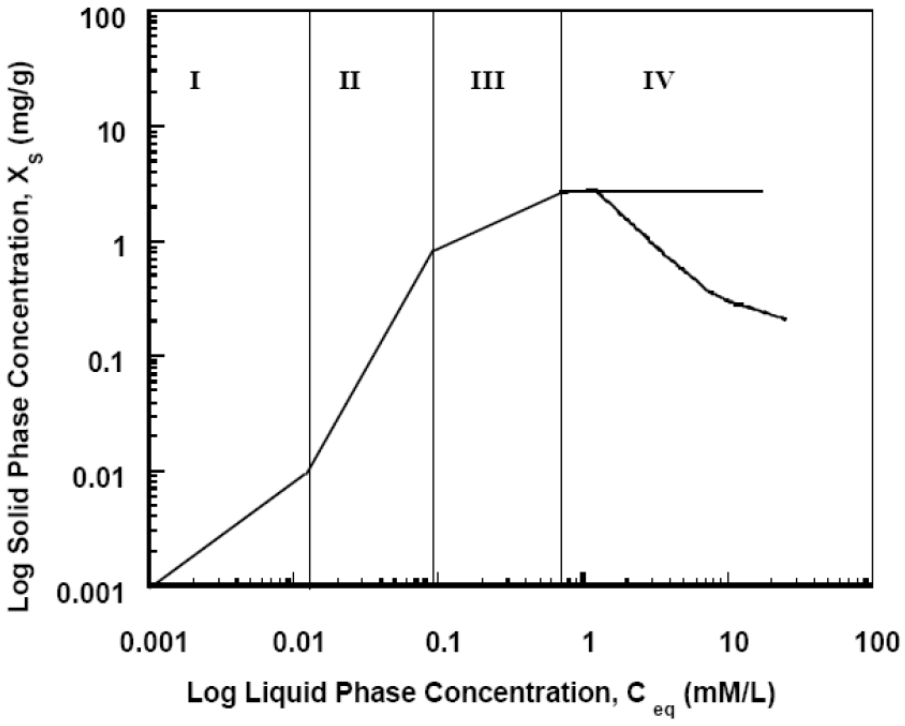

Figure 2.4. Schematic illustration of the four-regime adsorption isotherm

Figure 2.4 shows a log-log scale graph which describes a typical isotherm with four separated regions. In region I, Henry's law dominates the adsorption process with the linear correlation between adsorption and concentration. In region II, the surface aggregation of the surfactants generates the dramatically-absorbed rise. In region III, the rate of adsorption is slower than region II. In region IV, due to the concentration is above CMC, the adsorption rate is a plateau.

It is well accepted that the nature of adsorption curves is well explained for the first three regions [38, 39]. On the other hand, the underlying mechanism for region IV is not fully studied. It is ideally expected that the adsorption is kept constant beyond the CMC as at that point, the monomer concentration remains stable; but for some cases, this show a maximum adsorption due to some factors [40].

In case of the non-ionic surfactant, it has not been gained much attention in comparison with the ionic surfactants [41-47]. Langmurian or L2 [48] are often used to describe the adsorption isotherm of the non-ionic surfactants. It should also be noted that the most common isotherm has been utilized is the L4 type of Langmuir isotherm [49] instead of L2 simple. In addition, these surfactants have a tendency to be adsorbed physically compared to electrostatic or chemisorbed adsorptions. Unlike other surfactants, if there is a tiny change in any characteristic of the adsorbent such as concentration, temperature or molecular structure, the adsorption process will be greatly influenced. The reason is that the interactions between adsorbate-adsorbate and adsorbate-solvent produce the aggregation of surfactant in bulk and alter the packing and orientation at the interface.

2.2. Driving force of a flow or motion at the bulk and interface

2.2.1. Marangoni effect

The Marangoni effect is the flow of fluid caused by a gradient of surface tension. The mass transfer of this effect can be generated by the gradient of temperature or concentration. Generally, the fluid will move from the surface with low to high surface tension. In history, the first Marangoni flow [50] was considered by the tears of wine phenomenon (Figure 2.5). Generally, wine is a mixture of water and alcohol. When wine climbs to the side of glass due to capillary force, alcohol in wine evaporates faster than water then the higher surface tension is created. Due to the surface tension gradient, more wine from the bulk is dragged to the side of the glass and fall back by gravity.

Figure 2.5. Tear of wine

2.2.2. Benard-Marangoni convection flow

Benard–Marangoni convection (BM convection) was first discovered by Henri Benard [51] in the early of 20th century. In his experiment, a whale oil thin layer was located on a metallic plate and boiled at approximately 100^{o}C. The behaviour of extension in the horizontal direction was observed to be much bigger than its depth. Benard found that the hot liquid was rising up in the centre of the convective cell and down at the hexagonal boundaries. He concluded that the buoyancy in the bulk was the driving force to induce the flow. Based on linear stability analysis, Rayleigh [52] confirmed that the buoyancy certainly produced convective flow. Basically, the simple set-up of Rayleigh-Benard convection can be shown in Figure 2.6.

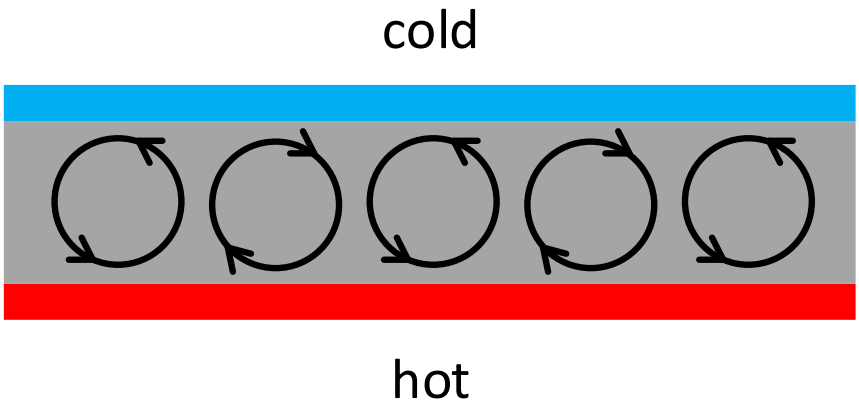

Figure 2.6. Schematic illustration of Rayleigh-Benard convection.

The fluid is located between two different plates with constant temperature. Initially, the fluid layer starts to be unstable due to the sufficient difference of temperature and becomes small flow perturbations. Due to the viscosity and thermal diffusion, the flow perturbations are only kept growing if the buoyancy forces acting on the fluid is sufficient to overcome.

The missing part of Benard flow was not discovered until 1956 when Block et al. [53] first performed the experiment and later on theoretical work by Pearson et al. [54]. In these reports, they let the top surface to be the free movement and found that the surface tension gradient is the second instability and the dominant factor in the thin layer. This is so-called BM convection (Figure 2.7). In general, the BM convection consists of both bulk and surface flow in comparison with only bulk flow description of Rayleigh-Benard convection. The temperature gradient acting on the free surface generated the surface tension's local decrease. This surface tension gradient induced forces away from the hot areas and brought the bulk flows and created surface deformation.

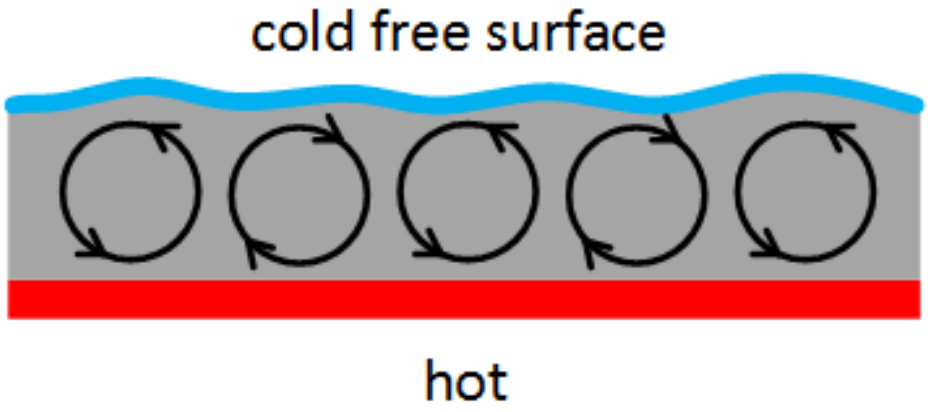

Figure 2.7. Schematic illustration of BM convection.

2.2.3. Thermal gradient-induced flow motion

Thermal gradient has been proved as one of the potential methods to actuate the motion of droplet or flow at the interface, especially in microfluidic applications [55]. Basically, there are two cases in term of generating flow by thermal gradient. First, the bulk flows or so-called BM flows are build up by the Marangoni instability inside the liquid layer when the temperature gradient is applied. Second, the surface flows are produced by the surface tension gradient along the surface. This temperature gradient is tangential to the liquid surface and can induce the surface flow from low to high surface tension areas. It should be noted that the surface flow cannot be isolated from the bulk motion which is much stronger. On the other hand, when the scale is down to micro, the surface tension becomes the dominant factor of the flow movement. Figure 2.8 shows the different form of Marangoni flow caused by the temperature gradient.

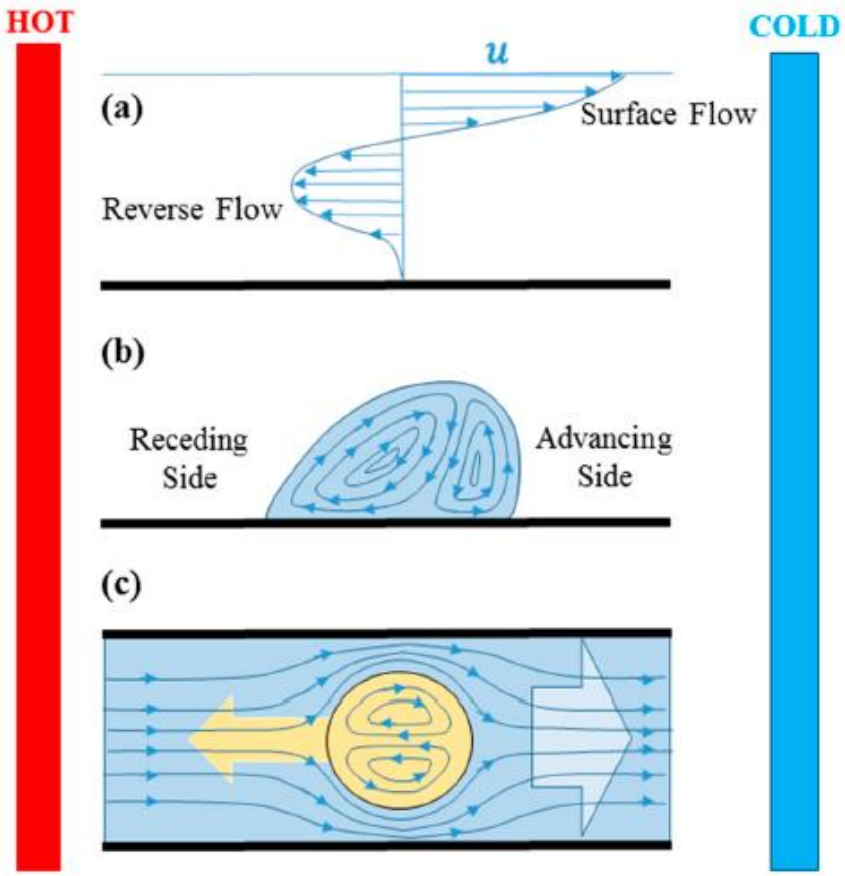

Figure 2.8. (a) Temperature-induced surface Marangoni flow, (b) Movement of the droplet on the solid substrate, (c) The carrier liquid moves to cold area whereas droplet moves reverse to hold mass conservation [55].

Theory

It is well-known that the Navier-Stoke equations [56, 57] are used to describe the motion of the fluid. These equations are associated with the temporal and spatial alteration of the velocity field of the fluid to the shear and normal stresses and the body forces. Generally, gravity is the only one body force without the presence of electrical and magnetic fields. In contrast, surface tension is just investigated in the boundary conditions as its impact only on the free surface of the fluid. Hence, surface tension balanced the tangential and normal stresses:

$$\hat{n}\overline{\overline{T}}\hat{n} = \gamma(\vec{\nabla}\hat{n})$$

$$\hat{n}\overline{\overline{T}}\hat{t} = \vec{\nabla}\gamma\hat{t}$$

T is the stress tensor, γ is the surface tension, $\hat{n}$ and $\hat{t}$ are unit normal and tangential vectors.

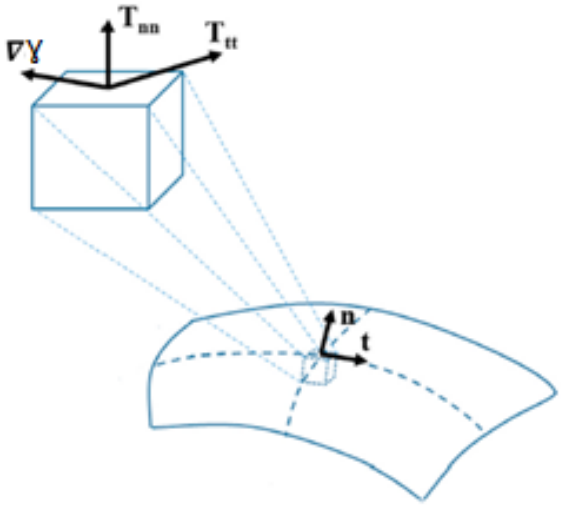

Figure 2.9. Components on a fluid surface element [55].

The above equations, in other words, state that the normal and tangential component of the hydrodynamic stresses has to be balanced with the portion of surface tension because of curvature and the tangential portion of the surface tension gradient, respectively.

The mechanism of generating fluid flow is to create the instability inside the flow by feeding the governing equations with a small perturbation. This perturbation can be varied in the characteristic of the flow such as temperature, pressure, the velocity with different frequency and magnitude. For example, the liquid films can be broken by the growth of these instability [58]. The spatial change of surface tension and mass

conservation in the presence of temperature gradient can induce circulations in which the amplitude and frequency are functions of temperature.

In one-layer liquid films, the thermocapillary motion which is based on the surface tension gradient with the temperature variation can be divided into two groups [59, 60]. First, Pearson [54] reported that steady-state convective instabilities (Marangoni convection form) were produced if the temperature gradient is perpendicular to the liquid free surface. Second, if not perpendicular but tangential, Smith and Davis [61] found that instabilities are the propagation of hydrothermal waves. The different states and critical conditions of these instabilities have been investigated by employing linear and non-linear stability analysis. In 1990, a phenomenon so-called fingering instability was found by Cazabat et al. [62] on spreading liquid films under Marangoni effect. This study showed that the liquid is capable of transporting above the meniscus level. Under this condition, the so-called fingering instability is the combination of Marangoni effect and hydrothermal wave propagation. Bowen et al. [63] reported that the velocity of the film is linked with the interfacial dynamic and the rupture of the film can be affected by the relationship between temperature and disturbance velocity.

It should be noted that such Marangoni-driven instabilities can be generated by evaporation. Saenz et al. [64] employed direct numerical simulation to simulate the dynamic of evaporation of liquid films or droplets. Sultan et al. [65] reported that the Marangoni stresses can be produced by the evaporation's heat transfer. The study also showed that while thermal-capillary and evaporation stabilized, the Marangoni effect destabilized the liquid. In another experiment, Kavehpour et al. [66] spread a silicone oil droplet on the solid surface and studied the evaporation-induced Marangoni instability. Three regimes of the droplet's dynamic characteristics have been named:

viscous-capillary, viscous-inertia-capillary and inertia-capillary. They found that these instabilities exist critical onset conditions and can be eliminated by manipulating the physical properties of liquid and substrate. The phenomenon so-called coffee ring effect is the first capillary effect on the evaporation of liquids. Deegan et al. [67] studied this phenomenon in 2000 by investigating the leaving colloids of a drying droplet on the solid surface. They stated that the mechanism of this phenomenon is the outward flow inside the droplet and the droplet pinning. A numerical study has been widely used to predict the mechanism of this process. Barash et al. [68] reported that there were different amounts of vortices can be formed inside the evaporating droplet. The numbers of vortices were depended on the relative conductivity of substrate and liquid droplet. Shih et al. [69], on the other hand, showed that the surface tension gradient induced the flow circulation. In this study, the evaporation rate increases with the rising temperature. In contrast, Marek et al. [70] found opposite results as evaporation coefficients decreases with when temperature are increased. Ajaev et al. [71] used the lubrication theory to develop a model for droplet evaporation. In this report, they just utilized a single equation to describe both macroscopic evaporation and microscopic liquid adsorption. Consequently, both evaporation and thermocapillary impact on droplet spreading. Once a droplet is being evaporated, while capillary aims to spread the droplet, the Marangoni effect actuates the flow inside the droplet. The evaporation is increased with the spreading process and the other way around with flow.

2.2.4. Marangoni effect-driven motion of the droplet

For the past few decades, controlling the surface energy gradient which induced the motion of the droplet at the solid/liquid interfaces has been received a great interest due to the various industrial applications such as coating, printing, photolithography

as well as microfluidic devices [1, 72]. Basically, the surfaces have been modified to possess a spatial non-homogeneous of surface tension by chemical reactions [2], chemical patterns [73, 74] or adsorption and desorption of surface active molecules [75]. As a result, these led to the alteration of contact angles and generated the non-mechanical droplet motion [76-78].

It should be noted that applying directly the external sources such as optical, thermal, acoustic or electric energy can produce the droplet motion without the surface modification [3]. The most disadvantage of these approaches was the need of external sources to induce and maintain the droplet transportation. In order to get rid of using external sources, the modification of solid substrate has been coming up as an alternative avenue to sustain droplet motion. Such modification can be split into two approaches: morphological and chemical treatments [3]. The first one consists of fabricating micro-structure and changing surface roughness. The latter, on the other hand, used chemical methods to alter the surface topography.

Chaudhury et al. [75] reported that a water droplet could climb uphill against the gravity. In order to obtain such gradient, the surface of a polished silicon wafer was treated by a vapour of decyltrichlorosilane, $Cl_3Si(CH_2)_9CH_3$. As a result, the surface possessed a hydrophobic gradient. Once a water droplet was located on the hydrophobic end, it moved toward the hydrophilic end. Although there are no Marangoni forces acting on the liquid, it should be noted that the movement was caused by the forces imbalance in which the opposite sides of the droplet maintained the surface tension gradient.

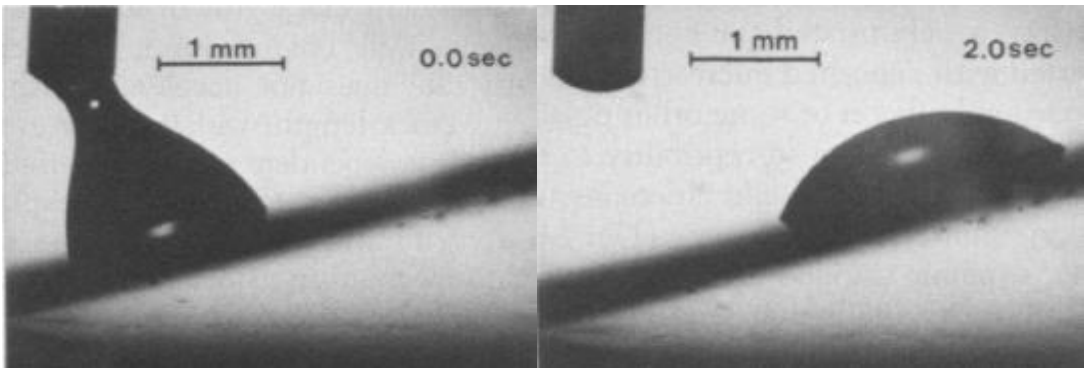

Figure 2.10. Uphill movement of a water drop on the gradient surface [75].

Instead of using a chemical method to modify the solid surface, Ichimura et al. [79] utilized the light source to induce the motion of liquid droplet. It is noteworthy that the outermost surfaces of the solid substrates are employed to calculate the surface free energies. Hence, light can be utilized to change the chemical structures of the outermost layer with the purpose of inducing and control many interfacial phenomena such as liquid crystal alignment [4], wettability [80], dispersibility [81]. Additionally, the gradient of surface energy in this method was spatially produced. As a result, the motion of liquid droplet was spatially controlled by the photoirradiation on the photoresponsive substrate. Eventually, the liquid droplet can move back and forth depending on the light source. On another attempt, Ito et al. [82] created a surface gradient by photodegradation approach. An alkylsilane self-assembled monolayer was tuned by using irradiation of vacuum ultraviolet light (wavelength 172 nm). In this report, the contact angle of water was controlled by the intensity and time of the light source. Consequently, the velocity of the water droplet motion was manipulated by adjusting the parameter of the light source.

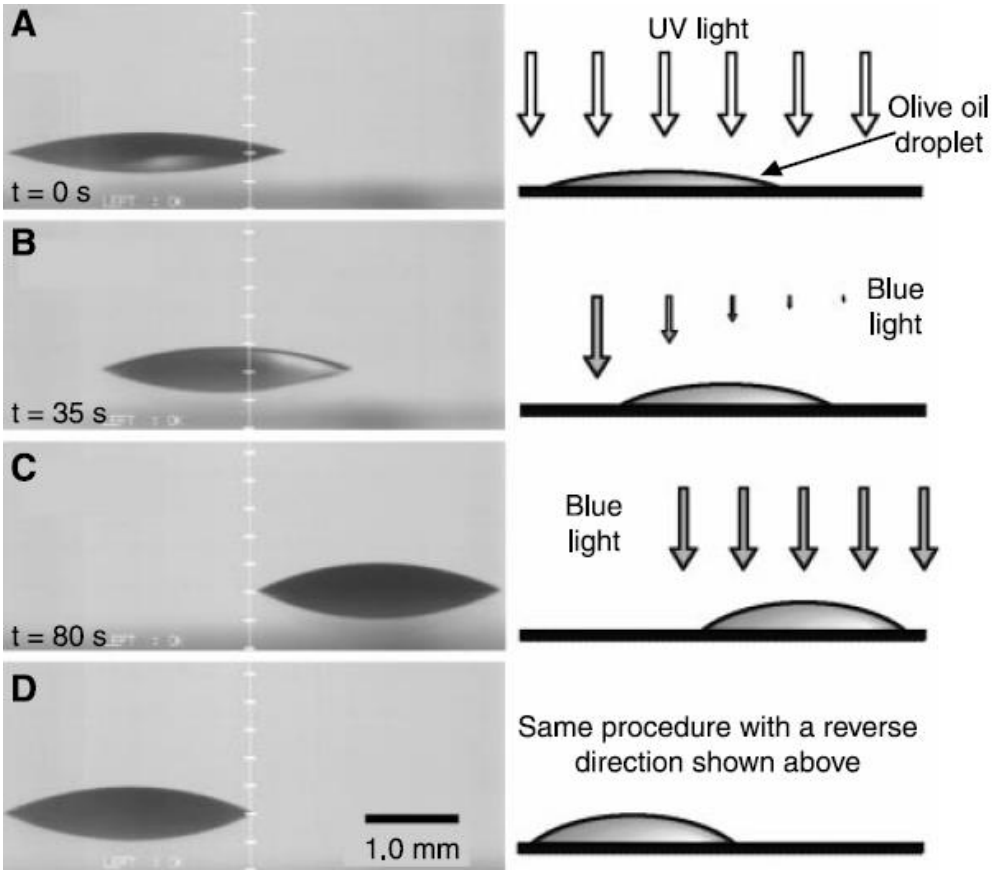

Figure 2.11. The motion of an olive oil droplet under the effect of light on a modified silica plate [79].

Recently, the emerging micro- and nanofabrication technologies have been developed rapidly. As a result, developing miniaturized fluidic devices is very challenging. Prins et al. [83] came up with an electrocapillary pressure-based fluid actuation. The mechanism of this movement was based on the electrostatic control of the solid/fluid interfacial tension. On the other hand, Gallardo et al. [5] used the redox-active surfactants combining with an electrochemical approach to control the motions aqueous and organic liquids on sub-millimeter and millimeter scales. In general, the spatial gradients of surface tension was generated by producing and consuming surfactant species at the opposite side of the electrode. Another potential approach in term of producing the gradient surface would be bipolar electrochemistry [84]. Dorri et al. [84] have reported that gradient electrodeposition of copper on the surface of the

bipolar electrode can induce the self-propelled movement of the water droplet. This method is easy to set-up and applicable to industry.

The non-mechanical motions of liquid droplet at the liquid interfaces are well-reported [85-92]. On the one hand, chemical reactions inside the object were the driving force to produce the self-propelled transportation. Ban et al. [85] reported a pH-dependent motion of the surfactant-loaded oil droplet in the aqueous medium. Generally, the alteration of the surface activity of the surfactant as a function of pH-induced the random movement of the oil droplet. On the other hand, the droplet needed the external sources to create a movement. Phan et al. [88] studied on the transportation of a microdroplet in oil layer between water/oil interfaces. By changing the number of cations and anions which was the fuel for the motion, the microdroplet can move up and down approximately 200 cycles.

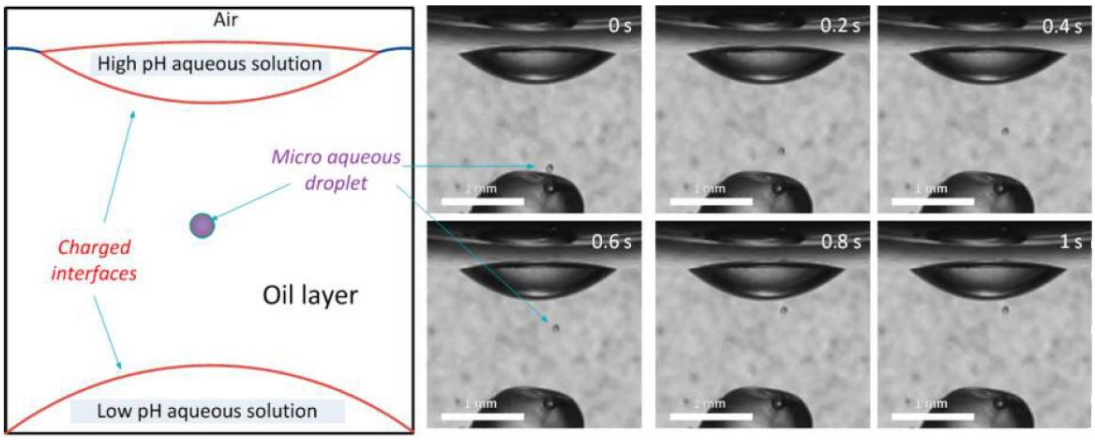

Figure 2.12. Rechargeable aqueous microdroplet [88].

Čejkova et al. [89] reported a simple system of decanol droplets motion with the alteration of sodium chloride concentration. This system is reversible as long as sodium chloride is kept adding to the other side of decanol droplet. Lagzi et al. [90] found that a small droplet of a water-immiscible organic solvent containing 20-60%

of 2-hexyldecanoic was induced to move toward the lower pH area. It is interesting that the droplet itself in the pH gradient could find the shortest way within a maze.

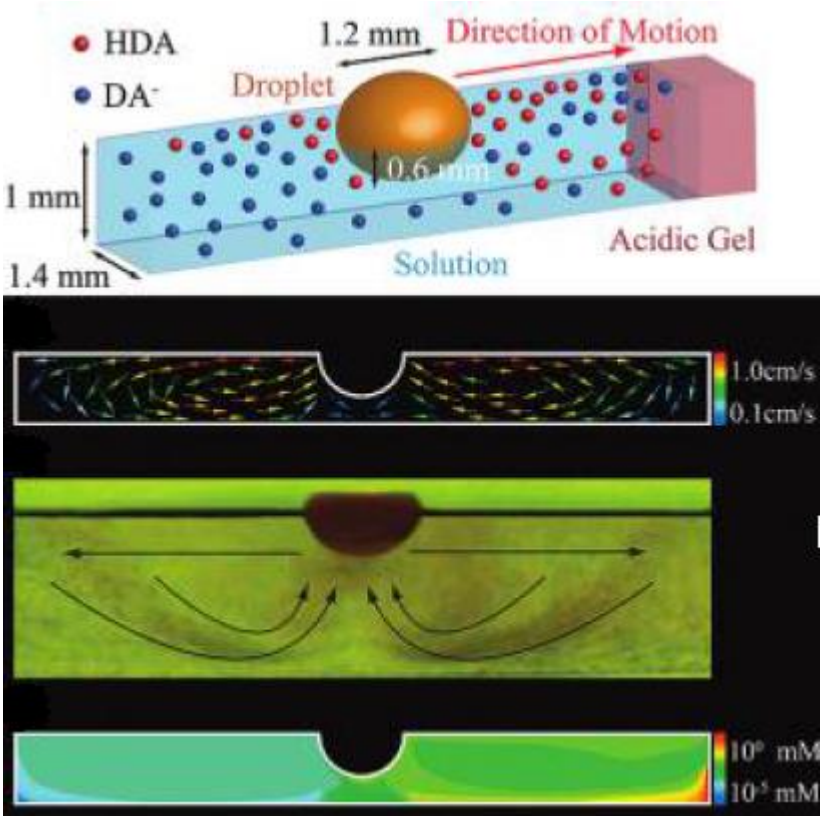

Figure 2.13. pH-induced droplet motion [90].

2.3. Gap in the knowledge

In the literature review, there are substantial researches related to the motion of a flow or an object in multi-phase. Most of the studies associated with either flow or object movement were driven by thermal factor has been done in solid surface treatment, bulk flow or evaporation. Recently, Kim et al. [92] reported a physico-chemical mixing phenomenon at the liquid-air and liquid-liquid interfaces. In general, it should be noted that none of them has proposed a clear observation and quantification for a thermal-induced surface flow.

In this thesis, such phenomena are studied by:

- Development of experimental procedure for observation and quantification of the phenomena.
- Development and verification of theoretical models to understand the underneath mechanism.
- Quantifying the influence of surfactant hydrophilicity on the phenomena.

Chapter 3 Methodology

A series of Triton surfactants (X-100, X-405, X-705) were used to investigate the surface flow at the air/water interface. The prosed model was applied to predict the nature of phenomena. Generally, there were two methods:

- Surface tension measurement (equilibrium and dynamic surface tension)
- Image analysis

3.1. Chemicals

3.1.1. Triton X-series

Three non-ionic Triton X-series were studied in this Thesis. No further purification is needed for these chemicals. Figure 3.1 and Table 3.1 show the structure and suppliers of the Triton X-series.

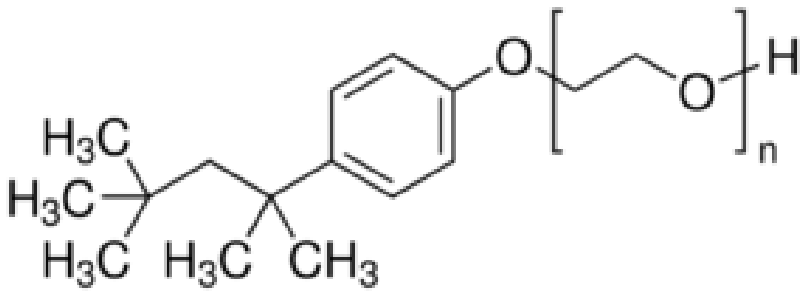

Figure 3.1. The structure of Triton X-series

Chemicals	Number of EO (n)	Suppliers	Purity
X-100	9.5	Sigma Aldrich	70% wt/wt in H_2O
X-405	35	Sigma Aldrich	70% wt/wt in H_2O
X-705	55	Sigma Aldrich	70% wt/wt in H_2O

Table 3.1. Number of EO groups, suppliers and purity of Triton X-series

3.1.2. Teflon ball

In order to observe the surface flow, the Teflon ball with a diameter of 0.79 mm was employed in this Thesis. It was purchased from the Hobby & Engineering Supplies. The properties of the Teflon ball are given below:

- No water absorption. Temperatures up to 288^{o}C.
- Not affected by any known acids or alkalies.
- Inert to chemical reaction.

Prior to use these balls, a massive washing was applied using ethanol and DI water to remove contaminants.

3.2. Apparatus

3.2.1. Surface tension measurements

3.2.1.1. Wilhelmy plate method

This famous technique is often used to measure the surface tension. In this method, a thin plate of glass or platinum will be put vertically and just halfway into the liquid [93]. Hence, the surface tension is given by Eq. 3-1.

$$\gamma = \frac{F}{p.\cos\theta_C} \qquad (3\text{-}1)$$

Where p is the perimeter of the plate in contact with the liquid phase and θ_c is the contact angle between the plate and the liquid phase.

This Thesis employed the tensiometer KSV Sigma 700/701 with Wilhelmy plate method to measure the equilibrium surface tension. The apparatus is depicted in Figure 3.2

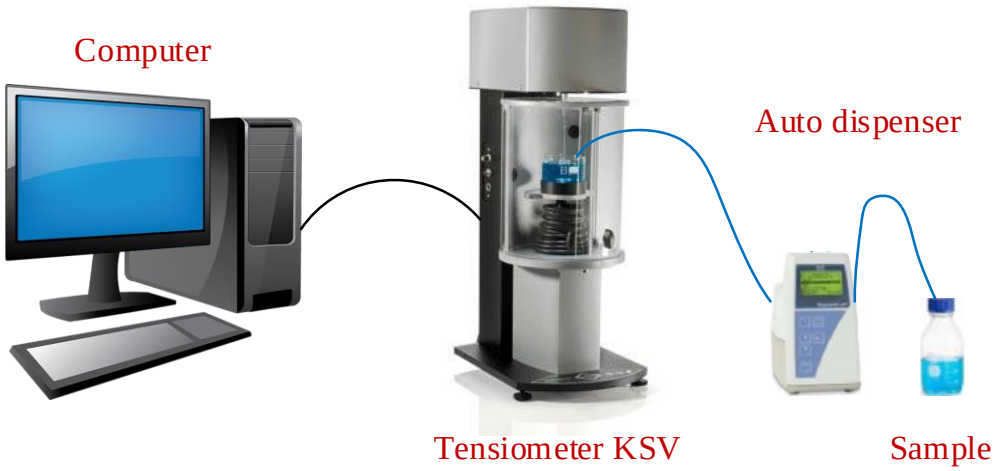

Figure 3.2. Equilibrium surface tension tensiometer (KSV 700/701)

3.2.1.2. Maximum bubble method

The maximum bubble pressure method or simply maximum bubble method is one of the most useful characterisations to measure the surface tension. The principal of this method is to measure the maximum pressure of a growing bubble at a capillary, which is immersed in the liquid phase. The whole process of the pressure variation inside a bubble is shown in Figure 3.3.

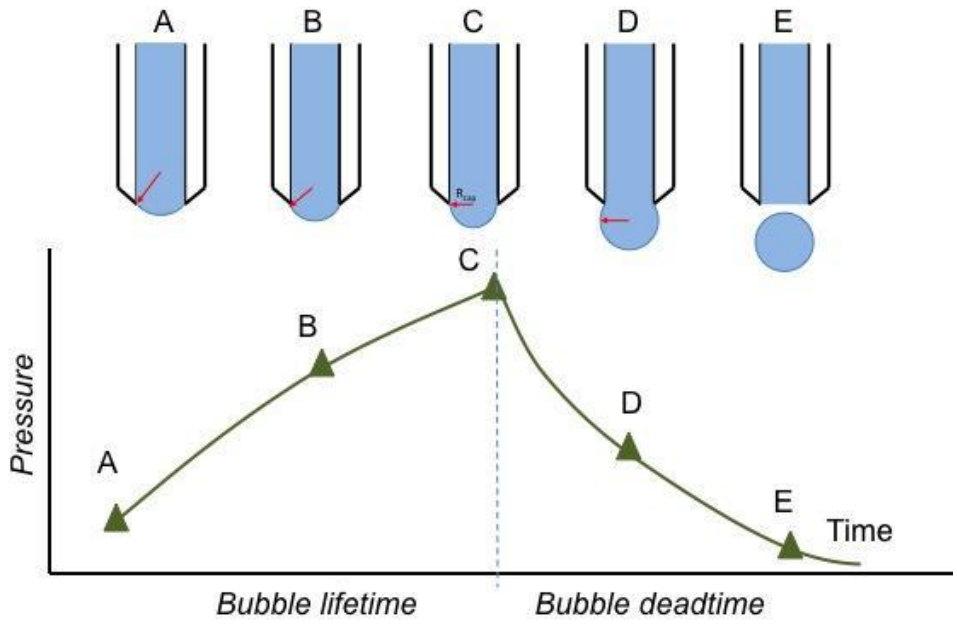

Figure 3.3. The principle of maximum bubble pressure method.

Firstly, the capillary is filled by a controllable-pressure gas and a gas/liquid interface starts to be created. Secondly, the pressure is kept increasing automatically until forming a hemisphere-shaped bubble which indicating the maximum pressure. The pressure is then declined gradually as the rise of bubble's size. Finally, the bubble is detached from the capillary and the process is kept going on by the alternative bubbles [94].

The dynamic surface tension of maximum pressure is calculated by Young – Laplace equation.

$$\gamma(t_{\max}) = \frac{p_{\max} - p_0}{2} R_{cap} \qquad (3\text{-}2)$$

Where p_{max} is the maximum pressure, p_0 is the hydrostatic pressure at the capillary and R_{cap} is the maximum bubble radius.

This method is performed on the MPT2 (Lauda, Germany, Figure 3.4) which has the 100 microns-diameter capillary. The dynamic surface tension is collected ranging from 10 ms to 10 s.

Figure 3.4. Dynamic surface tension tensiometer (MPT2).

3.2.2. Camera and Image analysis

3.2.2.1. Camera

The surface flow of surfactant layer is experimentally-difficult to observe. Instead of chasing the motion of the surface flow, a Teflon ball was located on the surface of surfactant solution. Once the Teflon ball moved, a camera was employed to record the videos of those movements. In this thesis, a DSLR Canon 550D with macro lenses (Figure 3.5) was used for all experiments.

Figure 3.5. Canon 550D and macro lenses

3.2.2.2. Image analysis

As showing in Figure 3.6, the recorded video was extracted to images with the frame rate of 30 FT/s. The software isOGG software which can be free downloaded on the Internet. These images were then applied in MATLAB codes using the edge detection function to track the position of the Teflon ball as a function of time. In order to understand the nature of the movement, two models were proposed to fit the obtaining position.

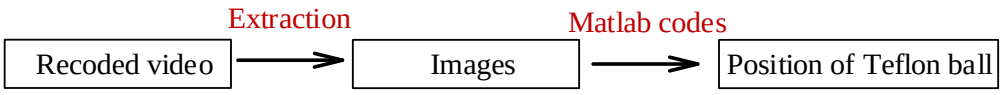

Figure 3.6. Analysis procedure

3.3. Summary

These methods are utilized to investigate the surface flow of the surfactant layer at the air/water interface. The equilibrium surface tension was employed to measure the CMC of the Triton surfactant solutions. On the other hand, the dynamic surface tension was applied to study the influence of temperature on the surface tension of Triton surfactant solutions. Finally and even more importantly, the image analysis method

was used to track the position of the Teflon ball which reflected the surface flow of surfactant layer.

Chapter 4 Influence of temperature on the surface tension of Triton surfactant solutions

4.1. Introduction

Non-ionic surfactants are utilized popularly in the industrial applications, such as foaming [95], cleaning [96], colloids and emulsion agents [97], stabilizer in oil processing [98], heat transfer [99] and mass transfer [100]. The impact of temperature variation on surface tension in these processes is significant as small temperature increment can alter the surface properties and induce the surface flow [101]. Triton series is one of the non-ionic surfactants using widely in the industry [102, 103]. In general, these surfactants structure has two parts. The first part is a tetramethylbutyl-phenyl group with the hydrophobic characteristic. The second hydrophilic part includes number of ethylene oxide (EO) groups, $(-C_2H_4O-)n$, which can be varied from 3 to 55. Benefiting from the different length in structure, Triton series can tune the hydrophobicity/hydrophilic balance. More importantly for most non-ionic surfactants, the hydrophilic part is also the EO groups [10].

While many research reported that the surface tension of water depends on temperature [104-106], the data for surfactant remains unknown. In literature, almost methods can be used to measure surface tension at room temperature but not for elevated one. For instance, CMC measurement is only effective at room temperature for the Wilhelmy method. The heating bath can be utilized to elevate temperature but the surface temperature would have a different value in comparison with bulk due to surface heat loss [107]. As a result, the closed cell is needed to saturate the air [106].

In this chapter, CMC of Triton solutions was first determined by the Wilhelmy method. Second, the maximum bubble method was employed to determine the surface tension at elevated temperature as it is simple to set up and obtain precise surface tension value. After reached the targeted temperature, it was kept constant during the measurement due to the bubble saturation with vapour.

4.2. Experimental

4.2.1. Procedure

The CMCs of three Triton solutions were determined at 25^{o}C by using KSV Sigma 701 tensiometer (KSV Instrument Ltd., Finland) with an automatic micro-disperser. The measurement was based on Wilhelmy plate method [108]. Consequently, each Triton solution was prepared at twice CMC to ensure the saturated condition. In addition to aqueous samples, samples with 1.5% and 3.5% NaCl (wt/wt) were also measured. The volume of solution was 50 ml. The surface tension was measured between 20^{o}C to 40^{o}C with 5^{o}C intervals using the maximum bubble pressure method (LAUDA MPT C) as presented in Figure 4.1. The solution temperature was maintained via the heated water bath. The temperature was monitored by a thermometer. After reaching the targeted temperature, the solution was connected to the machine for measuring the surface tension. At least three measurements were repeated at any given temperature.

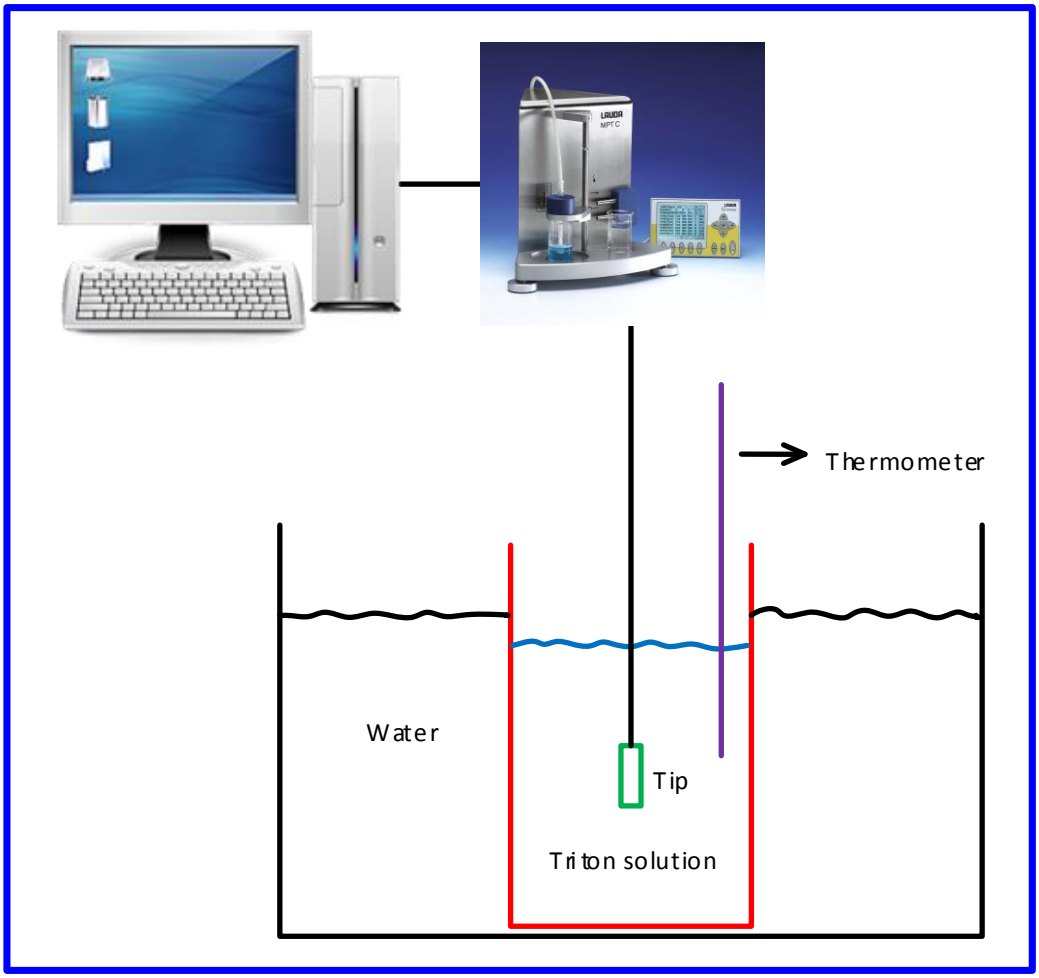

Figure 4.1. Experimental set-up

4.2.2. Results

4.2.2.1. Equilibrium surface tension of surfactants

The equilibrium surface tension of the three Tritons at 25°C is presented in Figure 4.2. The corresponding CMC are tabulated in Table 4.1. The obtained CMC is consistent with reported values for Triton X-100. The increased CMC with increasing number of ethylene oxide groups is consistent with reported trend [109]. Unlike ionic surfactants, the determination of CMC is not precise for Triton due to the long and gradual transition around the micellisation region. The lowest surface tension of Triton X-100

is slightly lower than that of X-405 and X-705. This also consistent with the reported trend of Triton series [109].

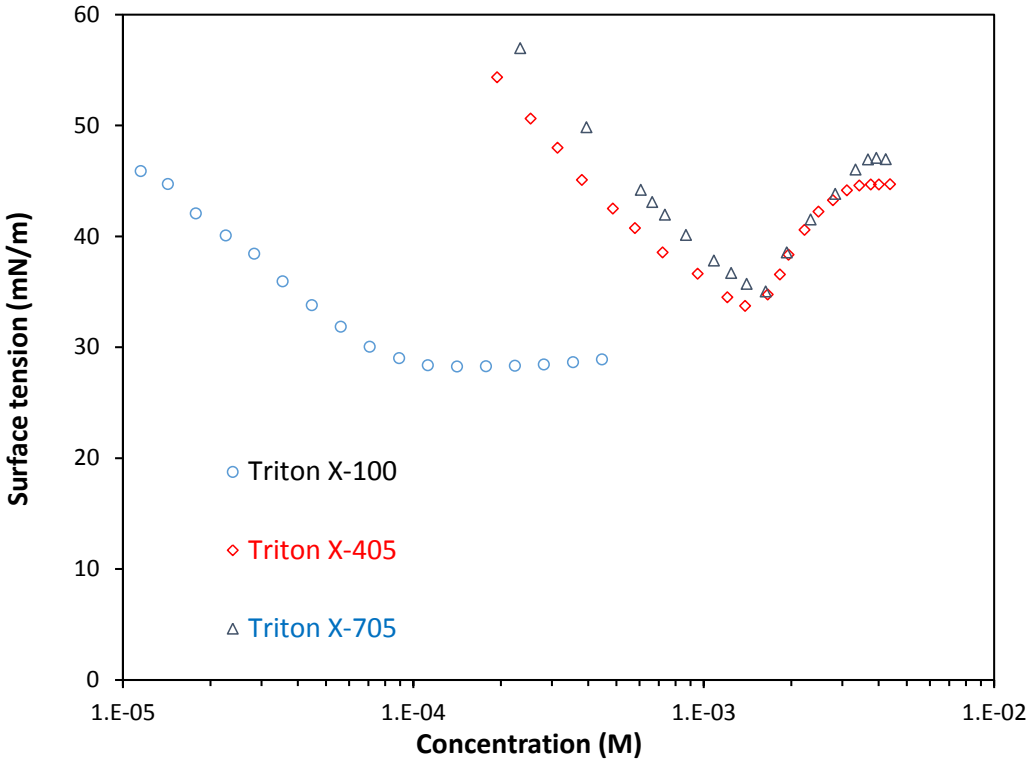

Figure 4.2. Equilibrium surface tension of different Triton solutions at 25°C

Table 4.1. CMC of different Triton solutions at 25°C

	Triton X-100	Triton X-405	Triton X-705
CMC (M)	~ 0.9 x 10^{-4}	~ 1.7 x 10^{-3}	~ 1.9 x 10^{-3}

4.2.2.2. Influence of temperature on the dynamic surface tension of three Tritons at twice CMC

Figure 4.3 shown the surface tension of three Tritons at a different temperature. It is obviously that dynamic curve was only appeared on Triton X-100. On the other hand, Triton X-405 and X-705 exhibited the fast adsorption with almost flat curves [28]. It should be noted that for all systems, the surface tension reached equilibrium approximately 10s.

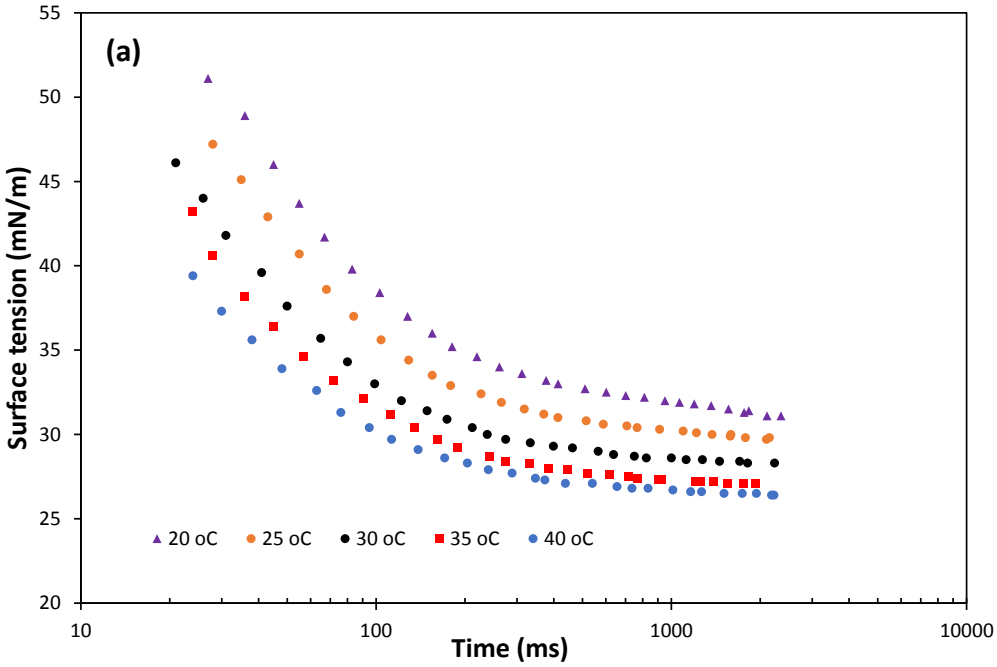

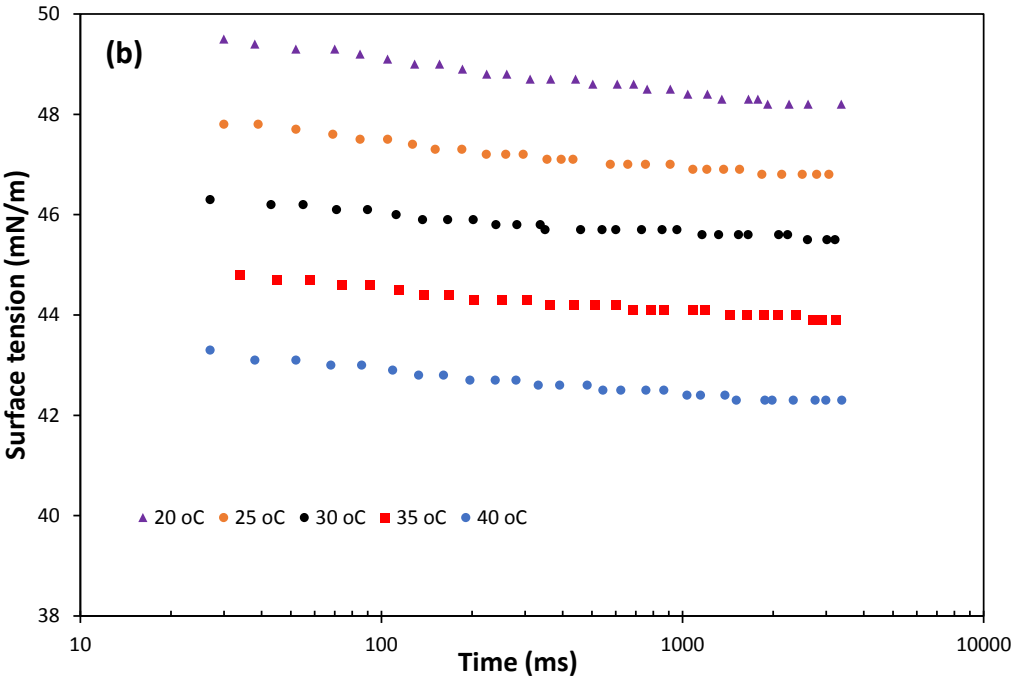

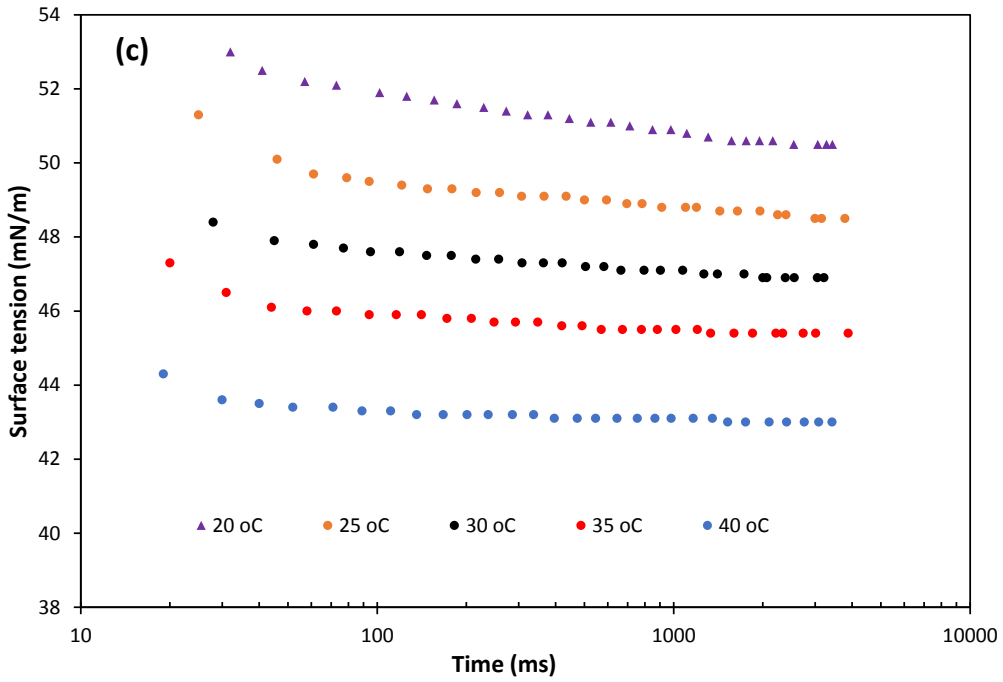

Figure 4.3. Dynamic surface tension of (a) Triton X-100, (b) X-405 (b), (c) X-705 at different temperature (without NaCl).

The surface tension versus temperature is plotted in Figure 4.4. For all surfactants, the surface tension decreased linearly with increasing temperature. The slopes of the

decrement are similar in the addition of NaCl. For Triton X-705, however, the additional NaCl reduce the slope slightly.

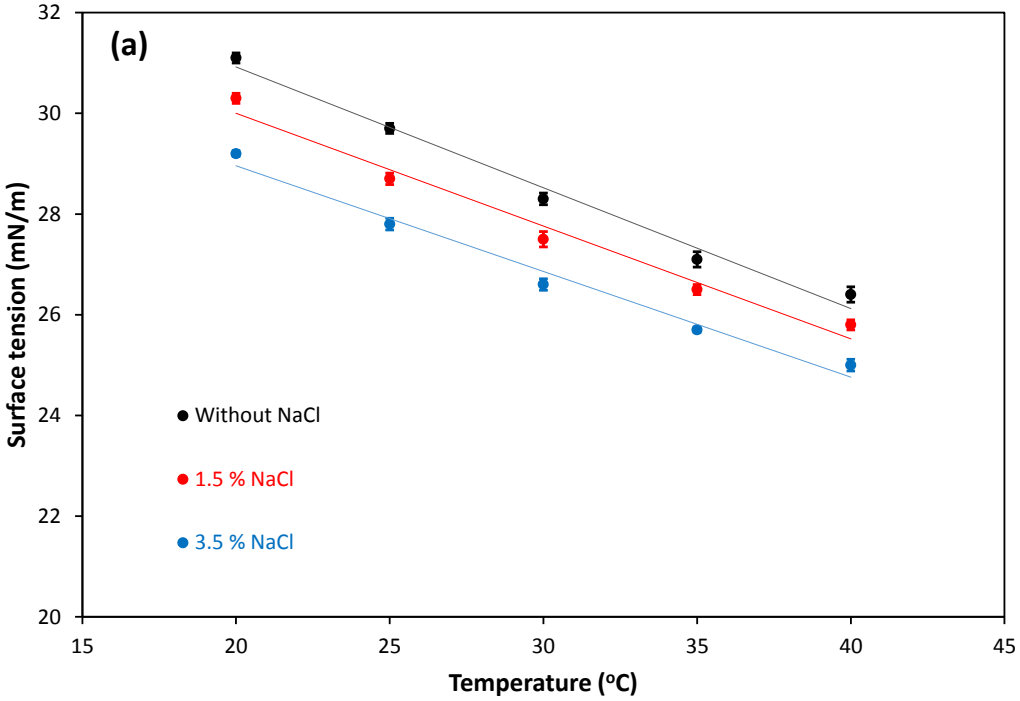

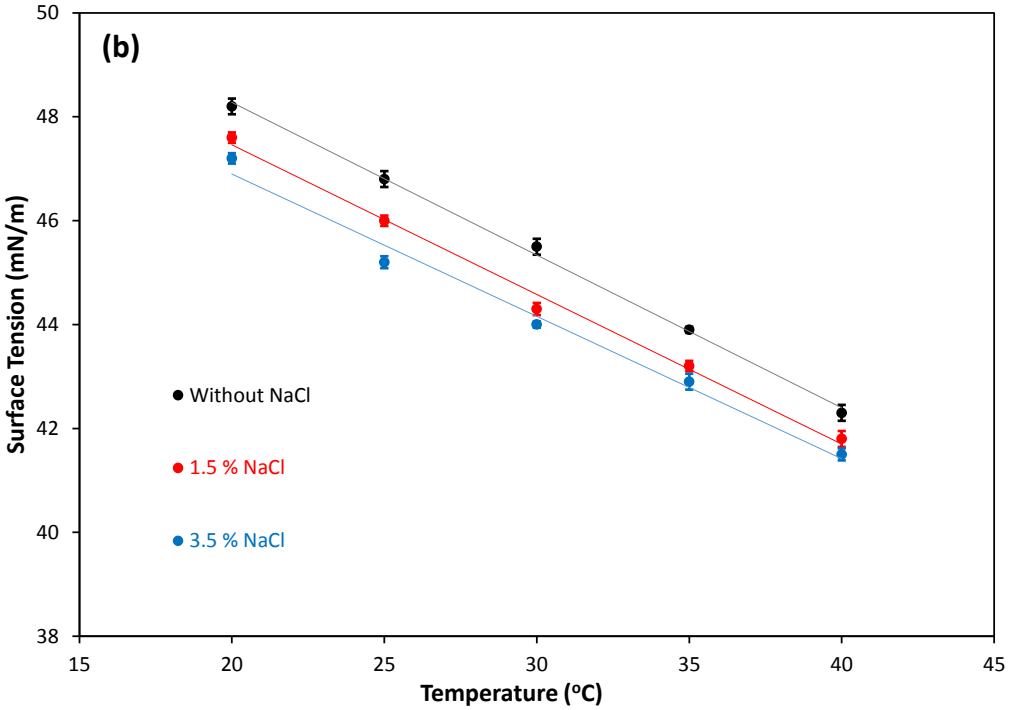

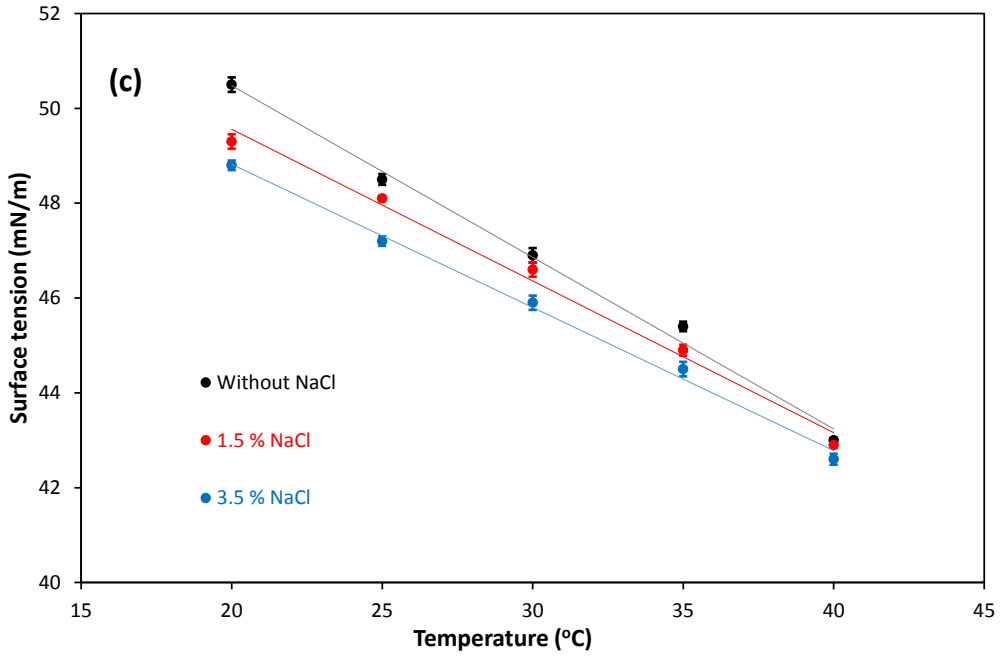

Figure 4.4. Surface tension as function of temperature at the different salt concentrations: (a) X-100, (b) X-405 and (c) X-705.

The slopes of surface tension- versus-temperature are tabulated in . This table can be used to predict the surface tension of Triton and NaCl at other temperature.

Table 4.2. The surface tension gradient against temperature

	Gradient (mN/m/K)		
	Without NaCl	1.5% NaCl	3.5% NaCl
Water	-0.158	-0.235	-0.245
X-100	-0.240	-0.224	-0.210
X-405	-0.294	-0.288	-0.274
X-705	-0.362	-0.320	-0.302

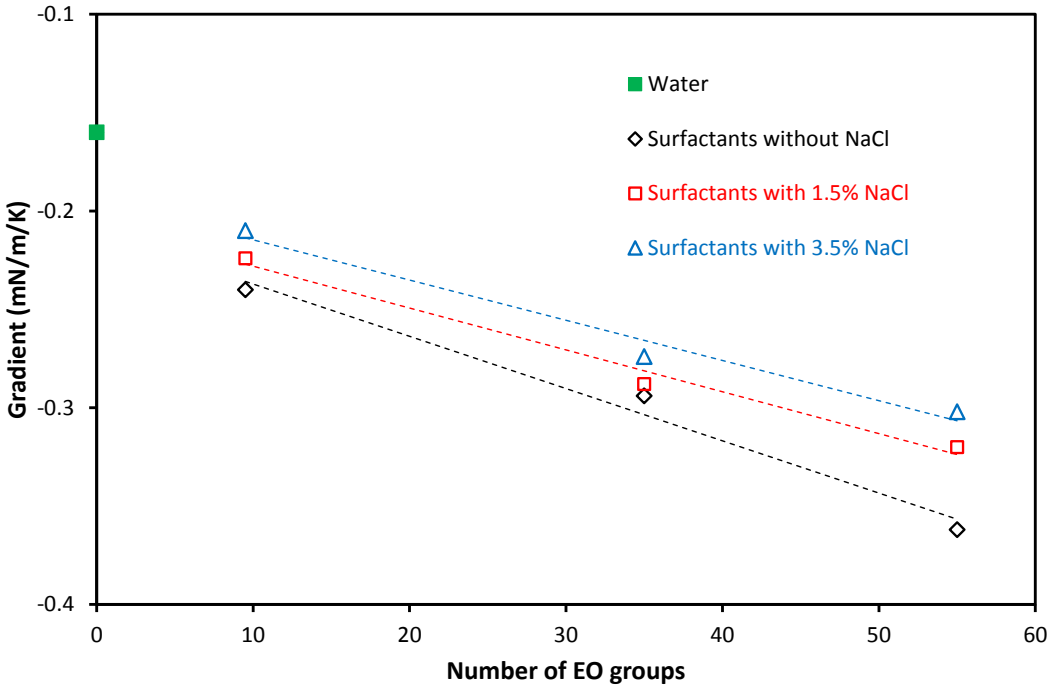

Figure 4.5. The gradient versus number EO groups on the surface.

As shown in Figure 4.5, the linear relationship verifies that H-bonds between water and EO is the dominant factor in the surface tension. The surfactant layer is more sensitive to the temperature changes than the pure water surface.

In literature, it has been predicted that H-bonds of liquid water will be broken once the temperature is increased [110, 111], and the surface tension is consequently reduced. Hyde *et al* [112] reported that an H-bond with the surrounding water molecules can be formed by each of the EO group. Consequently, the surfactant layer with the high density of EO groups produced not only an H-bond network with water molecules but also reduce the number of water-water H-bonds at the surface [113]. As a result, the influence of temperature on water is less profound than that on the surfactant layer [111]. Amongst the three surfactants, the Triton X-705, with 55 EO groups, can form the highest number of EO-water H-bonds per surface area and thus has a steepest

temperature-reduction rate. The results also demonstrated that EO-water H-bond is easier to break than the water-water H-bond, which is consistent with the weak polarity of the C-O bond within the EO groups.

The surface tension of all systems is decreased by the presence of NaCl. There is no apparent synergism between added NaCl and temperature for the investigated surfactants. However, the impact of NaCl is weaker for higher EO number. In this case, the dense H-bonds network around surfactant layer reduces the impact of NaCl.

4.3. Summary

Temperature has impacted differently on the surface tension of the three Triton surfactants. The more hydrophilic surfactant (more EO groups) is, the steeper thermal gradient will be. In addition to this, the thermal gradients of surfactants are higher than water. These behaviours are the results of the influence of temperature on H-bonds. The data can be used to predict the surface tension of these surfactant solutions for industrial processes. The quantitative relationship between the number of EO groups and reduction slope can be useful for other surfactants with a "poly-ethoxylate" structure, which is the common component for most industrial non-ionic surfactants.

Chapter 5 Experimental observation and theoretical development of the surface flow at the air/water interface

5.1. Introduction

In literature, the molecular arrangement has been well-known to generate unique characteristic on the adsorption layer of soluble surfactants at the air/water interface. The soluble surfactants layer is different from insoluble surfactants as it keeps an equilibrium with the bulk. As a result, in various interfacial processes, the underlying mechanism is based on the strong and flexible adsorption layer of soluble surfactant. In the turn of 20^{th} century, a well-known surface flow was reported based on the Marangoni effect [50]. This flow is generated by the gradient in the surface tension. Generally, the Marangoni effect co-exists with the bulk convection which is typically much stronger. Consequently, the dominance of surface flow can be only in small bulk volumes such as a tear drop of wine [50] or small oil droplet in water [85]. In big bulk flow, the bulk convection or so-called the Marangoni-Benard convection [114] dominates the surface flow.

Thermal changes have been well-known as a sensitive factor for surfactant adsorption [112, 115]. In addition to this, in Chapter 4, we have reported the linear relationship between temperature and the surface tension of non-ionic surfactants. As a result, a local temperature gradient on the surface can induce a surface flow. However, such phenomena have not been quantified systematically. This Chapter targets to develop experimental procedures and theoretical models to observe, quantify and verify the phenomena.

5.2. Experimental development

5.2.1. Procedure

Figure 5.1 shows the experimental setup. The Triton X-100 (n_{EO} = 9.5) solution was filled up in a half of a quartz cell (4x2x5 cm). The concentration was prepared at twice CMC to ensure the saturation for all experiments. A Teflon-coated Tungsten wire which was purchased from SDR Scientific (US) with an inner diameter of 0.2 mm was employed to produce the thermal field.

The wire was placed either under or above surfactant layer. Since the impact of thermal effect on surface flow is hard to observe, a floating Teflon ball was alternatively used to trace. The Teflon ball is inert and does not interact with water. In our theoretical development, there are just only surfactant tails attached to the Teflon ball. In our experiments, this 0.8 mm in diameter Teflon ball is the smallest one as we try to eliminate the volume effect on the phenomena.

The power sources are also changed either by DC or AC as both types of power source can generate the thermal gradient on the surface of surfactant flow. The current is managed as well to get the optimized condition. Finally, the distance between Tungsten wire and interface is also controlled ranging from 1 mm to 5 mm.

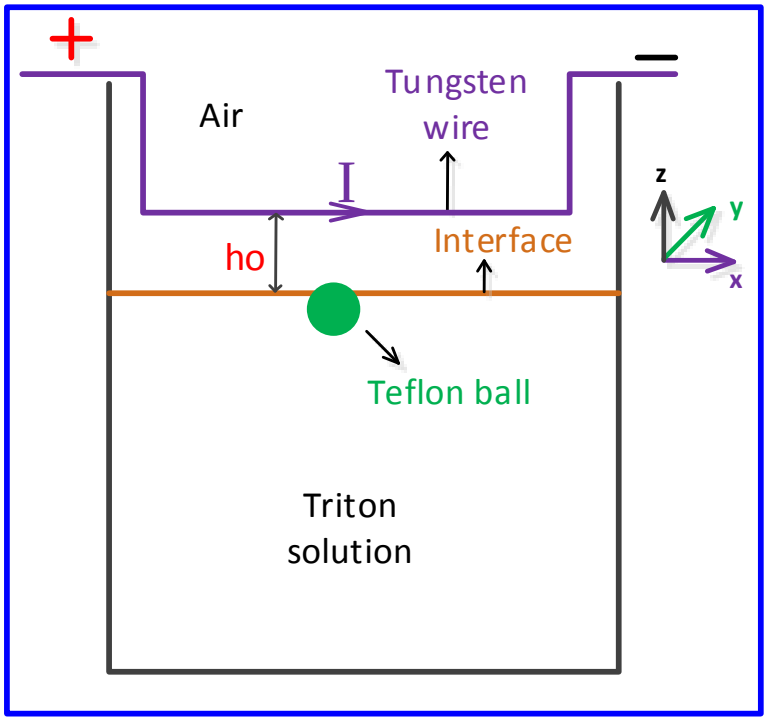

Figure 5.1. Experimental set-up of surface flow.

5.2.2. General observation

5.2.2.1. The wire under air/water interface

Once the power is turned on, the thermal effect generated a convection flow as shown in Figure 5.2. The gradient of this convection flow can induce the movement of the ball from the stationary position. As described in classical Bernard-Marangoni flow [116], the thermal convection may interfere with the surface gradient. It should be noted that the underlying mechanism around the ball is complex. In this thesis, the above case was selected to analyse as it is free from convection.

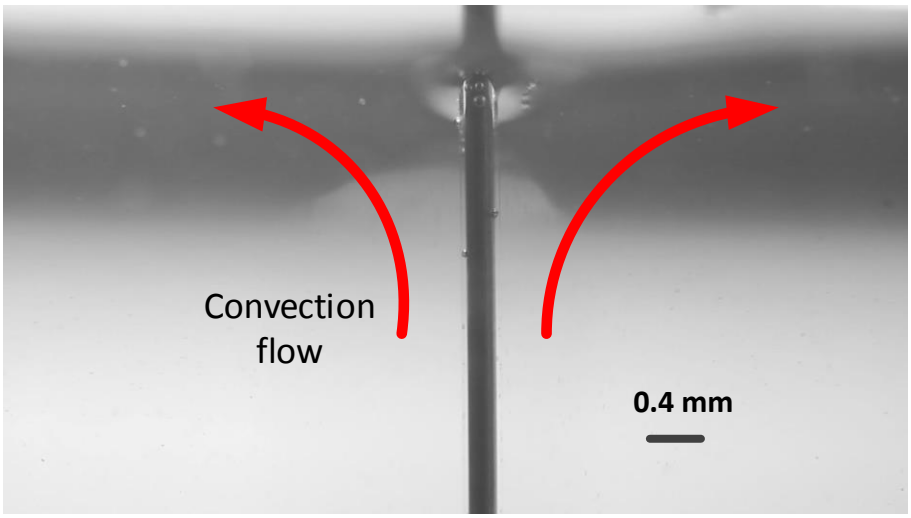

Figure 5.2. Thermal effect-induced convection flow (side view).

5.2.2.2. The wire above air/water interface

When the power was applied, the floating Teflon ball transported perpendicularly to the electrical current in the *y*-direction as showed in Figure 5.1. The movement of the ball was always further away from the wire no matter what the initial position of the ball can be. It is noteworthy that the insulating coating layer of the wire prevented the impact of electrical current. The horizontal position of the ball (Figure 5.3) was then obtained by image analysis as a function of time.

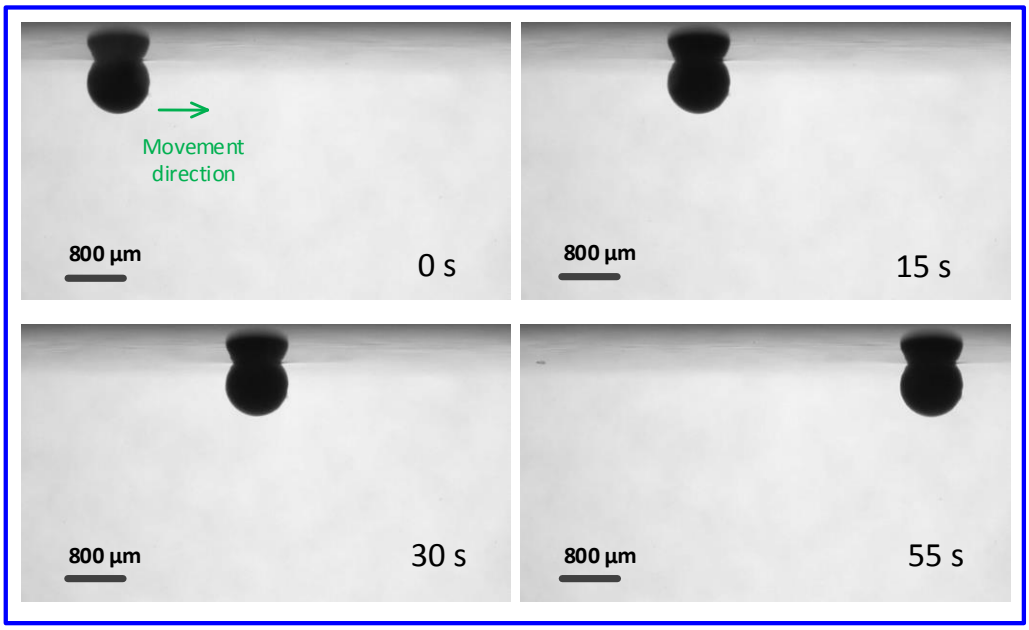

Figure 5.3. Raw images of ball motion

The experiments were also repeated by changing the surfactant solutions such as pure water, sodium dodecyl sulfate (SDS), cetyltrimethyl ammonium bromide (CTAB) but there was no movement occurred.

In order to trace the temperature gradient on the surface, a thermal camera was used to record the thermal map (Figure 5.4). The the maximum difference was ~8 °C and localized near the centre.

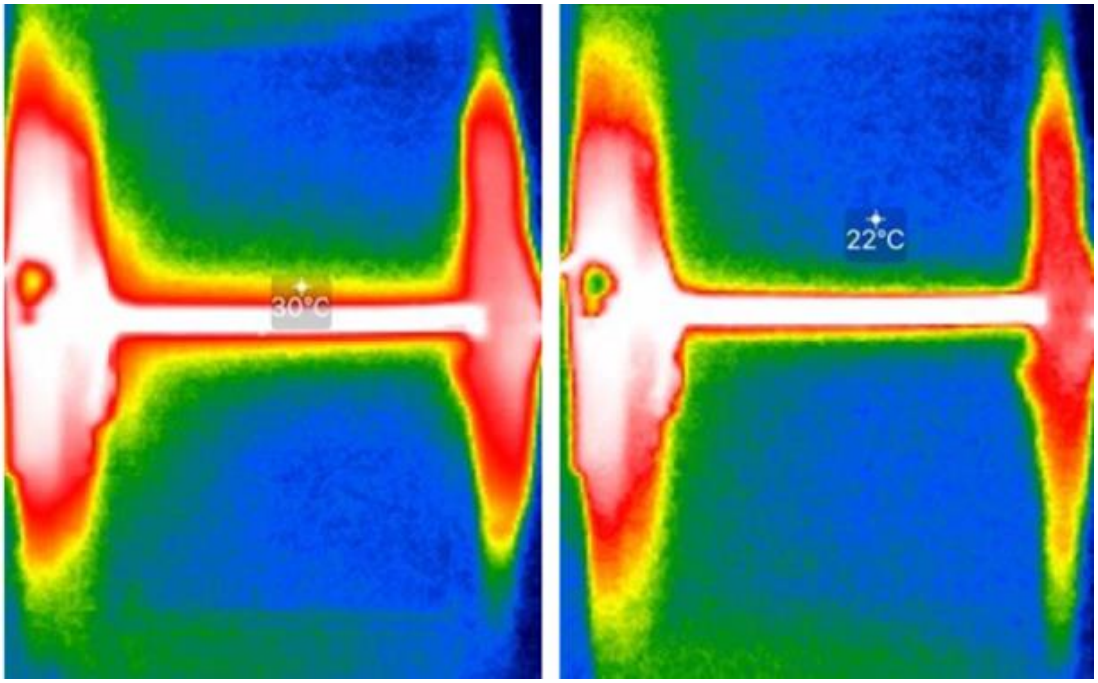

Figure 5.4. Thermal images of surface temperature: (left) spot temperature near the wire position and (right) spot temperature at ~5 mm from the wire position.

5.3. Theoretical development

5.3.1. Proposed model

5.3.1.1. Driving force

The relative tension of the interfacial layer was utilized to explain the transportation phenomenon. The forces acting on the ball were employed in the model by the driving force and friction force. The model was then fitted with experimental data to reveal thermal constant of surfactant layer and the nature of the friction force. Once a surface tension gradient is produced around the ball, the surface force induces the ball into high tension area. The similar phenomenon has been reported on the small liquid droplet movement induced by chemotaxis [89].

The surface force for the spherical ball is given by the gradient of the surface tension [117] as shown in Figure 5.5:

$$F_a = -\frac{d\gamma(y)}{dy}\cos(\beta)A_a \qquad (5\text{-}1)$$

Where $\gamma(y)$ and A_a (mm^2) is the local surface tension at position y and the surface area of the contacting surface between ball and water, respectively. In the above equation, β is the contact angle between air/water surface and horizontal axis. The angle is given by [117]:

$$\beta = \theta_a - \varphi \qquad (5\text{-}2)$$

Where θ_a is the contact angle between air/water surface and the solid material, and ϕ is the "immersion" angle.

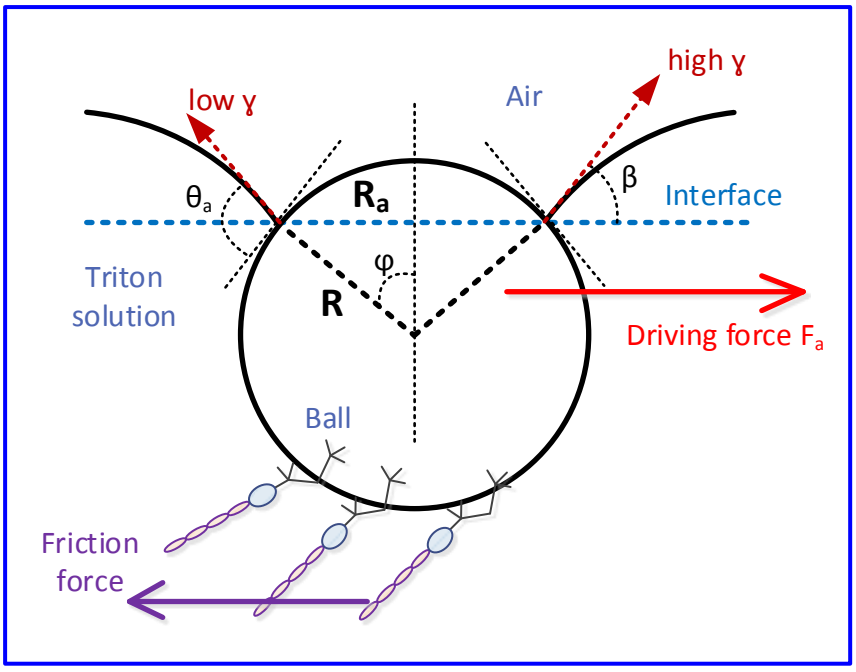

Figure 5.5. Schematic illustration of floating ball on surfactant solution

Since the relationship between air/water surface tension and temperature has been reported as a linear function [104, 118], the local surface tension is related to the local temperature:

$$\gamma(y) = A_1 - A_2 T(y) \qquad (5\text{-}3)$$

Where A_1 and A_2 are positive constants.

The value of A_2 varies with the molecular nature and adsorbed concentration of the surfactants and can be determined experimentally. From Eq. (2) and (4):

$$F_a = A_2 A_a \cos(\beta) \frac{dT}{dy} \qquad (5\text{-}4)$$

Since the hotwire generated the uniform heat flux in all direction on the *xy*-plane (Figure 5.6), the heat flux is given by:

$$q(r) \propto -A_r \frac{dT}{dr} \qquad (5\text{-}5)$$

Where $q(r)$ is the heat flux at the radial distance r, and A_r is the surface area of the cylinder around the wire.

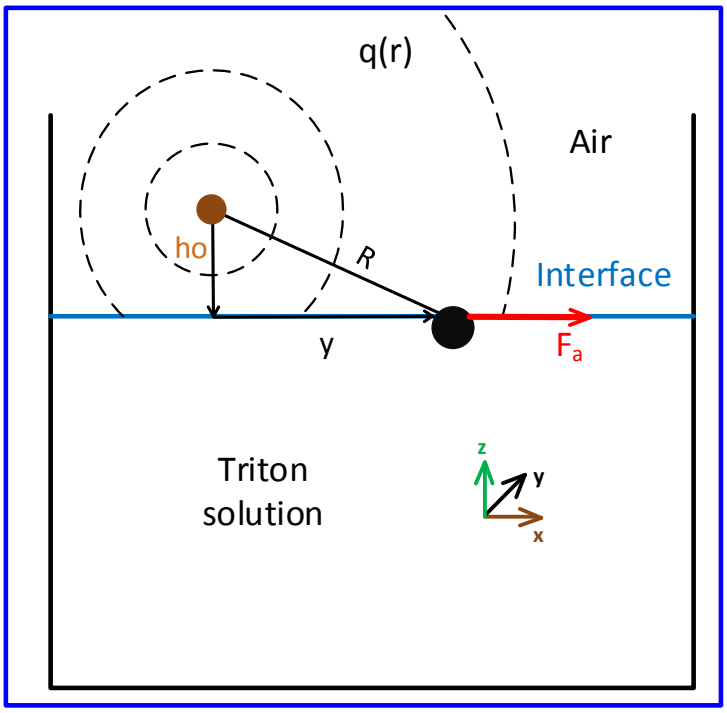

Figure 5.6. Elemental force analysis of movement

Since *q(r)* is constant and A_r is proportional to $2\pi r$, the above equation yields:

$$\frac{dT}{dr} = C_T \frac{1}{2\pi r} \qquad (5\text{-}6)$$

Where C_T (K) is a constant accounting for the heat transfer to air. The radial distance from the wire is related to horizontal distance, *y*, by:

$$r = \sqrt{y^2 + h_o^{\,2}} \qquad (5\text{-}7)$$

Where h_0 is the vertical distance from the wire to surface, which remains constant throughout the experiments. As a result, the temperature gradient is given by:

$$\frac{dT}{dy} = \frac{dT}{dr}\frac{dr}{dy} = \frac{C_T}{2\pi}\frac{2y}{\sqrt{y^2 + h_o^{\,2}}}\frac{1}{\sqrt{y^2 + h_o^{\,2}}} \qquad (5\text{-}8)$$

Hence, equation (2) reduces to:

$$F_a = \frac{C_T A_a A_2}{2\pi} \cos(\beta) \frac{y}{y^2 + h_o^{\,2}} \qquad (5\text{-}9)$$

It should be noted that A_a (m^2) and β are varied with surfactants, and are determined experimentally. The value of A_2 (mN/m/K) is also determined independently from the slope of surface tension-versus-temperature profile.

5.3.1.2. Friction mechanism

While the F_a is the driving force, the friction slowed down the movement of the ball. In this thesis, two friction mechanisms are considered: (i) "dry" friction or (ii) lubricated sliding friction [119]. While the friction is independent on velocity in the dry model, it is on the other hand directly proportional to velocity on the lubricated case.

In case of a "dry" friction, a drag force acts against the movement with a constant deceleration, a_f^i (m/s^2) [119]. Hence, the total acceleration of the ball is given as:

$$a(t) = \left[\frac{1}{m_a} \frac{C_T}{2\pi} A_a A_2 \cos(\beta) \right] \frac{y}{y^2 + h_o^{\,2}} - a_f^i \qquad (5\text{-}10)$$

The equation is simplified by introducing E_{ff} (m^2/s^2), which is defined as:

$$E_{ff} = \frac{1}{m_a} \frac{C_T}{2\pi} A_a A_2 \cos(\beta) \qquad (5\text{-}11)$$

For lubricated friction, the friction component, a_f^d, is given by[119]:

$$a_f^d = C_d v \qquad (5\text{-}12)$$

Where C_d is the friction coefficient (s^{-1}) and v is the transient velocity (m/s). The total acceleration, in this case, is as given:

$$a(t) = E_{ff} \frac{y}{y^2 + h_o^2} - C_d v(t) \qquad (5\text{-}13)$$

Hence, the motion is fully described by a system of two ODEs:

$$\begin{cases} \dfrac{dy(t)}{dt} = v(t) \\ \dfrac{dv(t)}{dt} = a(t) \end{cases} \qquad (5\text{-}14)$$

Where $a(t)$ is given by either Eq. 5-10 or Eq. 5-13. The initial conditions, when the power was turned on, are given by:

$$\begin{cases} y(t) = y_0 \\ v(t) = 0 \end{cases} \qquad (5\text{-}15)$$

Where y_0 is the initial horizontal position.

A numerical scheme was developed to solve the above system of ODEs and then fit the experimental data. Euler's method with a step-size of 0.03 s was employed. In the first model, the two parameters are E_{ff} and a_f^i. In the second model, the two parameters are E_{ff} and C_d. The error is calculated by:

$$\varepsilon = \frac{1}{n} \sum_{i=1}^{n} \frac{\sqrt{\left(y_i^{\exp} - y_i^{\mathrm{mod}}\right)^2}}{y_i^{\exp}} \qquad (5\text{-}16)$$

Where n is the number of experiments, $y_i^{\exp}$ and y_i^{mod} are the experimental and modelled values.

5.3.1.3. Modelling assumption

In our model, the heat diffusion from the wire into the surface when the power is turned on is assumed to act immediately. Consequently, the dynamic mechanism of the movement is negligible.

5.3.2. Modelling verification

Figure 5.7 exhibits the modelling results for both cases. It is clear that the experimental data was fitted successfully to the dry friction model with a smaller ε. In contrast, the data was described unsuccessfully by the lubrication model. It is obvious that the lubrication model failed near the end of the motion in which depicted a continuing increment against the experimental plateau. As a result, the dry friction is confirmed to be the governing mechanism of the movement.

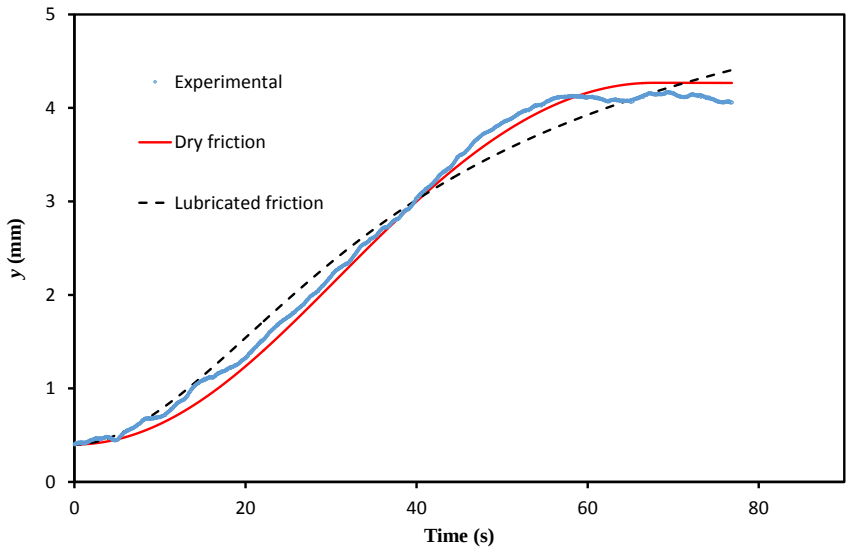

Figure 5.7. Modelling motion of the floating ball at h_0 ~ 2.5 mm for twice CMC of Triton X-100 solutions.

The fitting parameters are tabulated in Table 5.1.

Table 5.1. The fitting parameters of the prosed models.

h_0	Dry friction model			Lubricated friction model		
(mm)	a_f^i (m/s^2)	E_{ff} (m^2/s^2)	ε (%)	C_d (s^{-1})	E_{ff} (m^2/s^2)	ε (%)
1	0.662	0.165	10.5	0.073	1.126 x 10^{-11}	13.4
2.5	0.662	0.294	5.63	0.073	5.76 x 10^{-11}	6.26

It is obvious in Table 5.1 that a_f^i is independent on h_0. Consequently, the model has been further confirmed the initial assumption that the molecular nature of the contacting layer, not the driving force, had an impact on the friction coefficient. The simplification in the model was the cause of the change in E_{ff} value. Moreover, the model ignored the significance of the ball dimension. It is necessary to employ a complex simulation, such as Discrete Element Method [120] to fully address these issues.

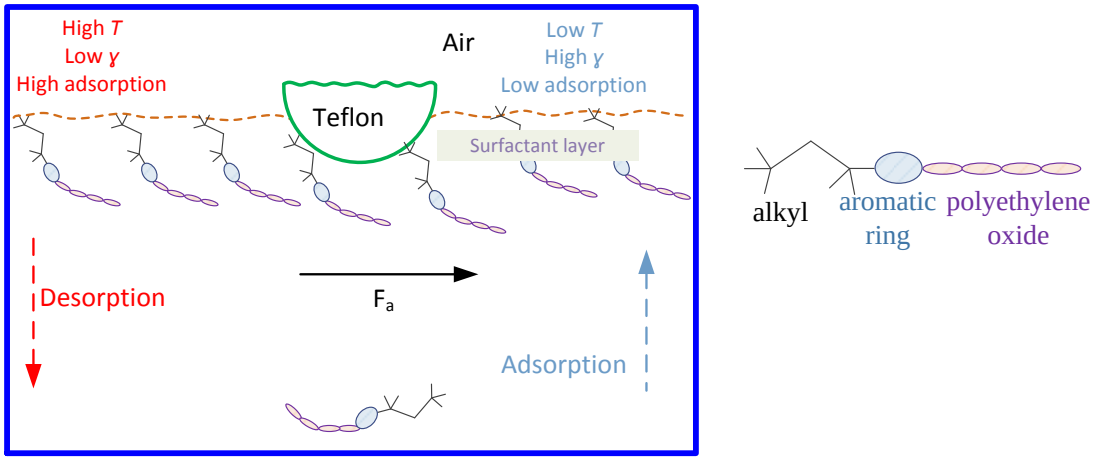

Figure 5.8. Microscopic nature of the ball movement.

As shown in Figure 5.8 the microscopic structure of the surfactant can be used to explain the transportation of the ball. The desorption at the higher concentration and the adsorption at the lower concentration were utilized to describe the balance of the surface movement. Lovass *et al* [121] reported the similar surface flow of surfactants. It can be seen in Figure 5.3 that the ball and the surfactant flow were moved together due to the adhesion between Teflon and the highly hydrophobic surfactant tail. It should be noted that the phenomena did not happen in case of alternative solutions such as SDS, CTAB and pure water as well. It is noteworthy that the benefit of the long hydrophilic EO groups help Triton X-100 forming a strong network of H-bonds near the interface [112]. As a result, the lateral motions along the surface of SDS and CTAB would be less crucial than Triton.

5.4. Summary

The observation and analysis of thermal-induced surface flow were carried out by using the floating Teflon ball and a non-ionic surfactant (Triton X-100). A simplified model was applied to quantify the flow. Since the monolayer movement was the cause of molecular nature of motion, the dry friction model governs the friction. It is foreseeable that the existence of this phenomenon could occur with other non-ionic surfactants. In the next chapter, further study was performed to investigate the impact of molecular structure on the phenomena.

The phenomenon can be applied for many micro- and nano-fluidic applications, where the dominant force is the surface force. For instance, the multi-phase systems in microfluidic devices can be manipulated by utilizing the thermal-induced surface flow.

Chapter 6 Influence of surfactant hydrophilicity on the surface flow at the air/water interface

6.1. Introduction

A chemical/physical property such as concentration, temperature or modified solid surface can be employed to generate the non-homogeneous surface in which a surface flow can be created [122]. In chapter 5, it has been found that a surface flow which could induce a floating ball was driven by a thermal gradient on air/water interface. In this study, three Tritons (X-100, X-405, X-705) with added salt were employed to investigate the more obvious insights of the phenomena. The molecular nature of the three Tritons was depended on the number of EO groups. The more numbers of EO groups it has, the more hydrophilic property is. Various industrial applications have been using these surfactants [96, 103, 123, 124].

There are two parts in this study. The first one is to measure experimentally the surface tension of solution at different temperatures. This part has been done in chapter 4. The second part is to monitor and analyse the ball transportation at different solutions. The modelled analysis results were utilized to address the influence of molecular structure on the mechanical- and thermal-responses of the surfactant layer.

6.2. Experimental

The experimental set-up in Chapter 5 was used in this study. Twice CMC of three Triton solutions with 3.5% NaCl was utilized one by one and put in a quartz cell. It is interesting that the Teflon ball did not move without the presence of salt.The experiments were repeated exactly same with the wire-above case in Chapter 5.

6.3. Analysis

6.3.1. Influence of temperature on surface tension

It is well-accepted that both H-bonds [110] and surface tension [125] is the linear function of temperature (Figure 6.1). Surfactant molecules of non-ionic surfactants break the water-water H-bond network near the interface [126].

The H-bond network of Triton surfactants at the surface is dominated by the water-EO or EO-EO H-bonds [127]. As the temperature increases, it is expected that the bonds network is reduced gradually as with water-water H-bonds. Hence, the linearity between surface tension and temperature is expected.

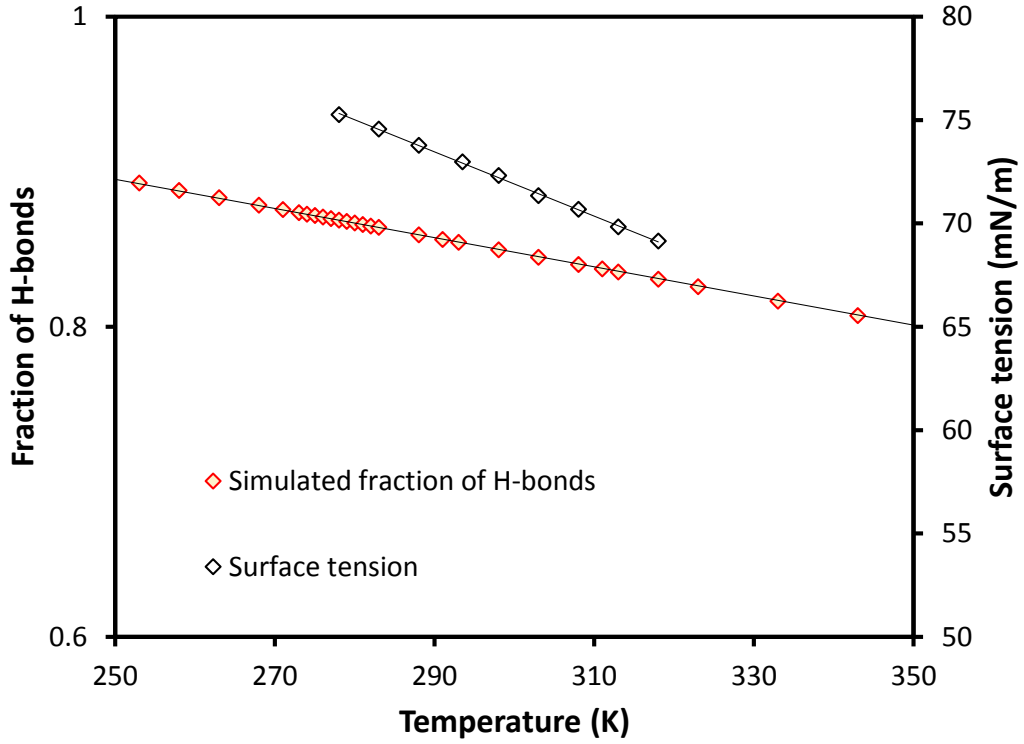

Figure 6.1. The influence of temperature on H-bonds fraction [110] and surface tension [125] of water.

The influence of temperature on surface tension will be proportional to number of EO:

$$\frac{d\gamma}{dT} = \frac{d\varepsilon}{dT}\Gamma_s n_{EO} \qquad (6\text{-}1)$$

Where ε is energy per EO group (J/mol), Γ_s is surfactant concentration at the interface (mol/m^2) and n_{EO} is number of EO groups per surfactant molecules.

In chapter 4, the slope of $d\gamma/dT$ has been experimentally gained for each surfactant. The validation of the thermal linearity and Eq. (6-1) will be based on these data. The slope was then used to model the ball motion.

6.3.2. Influence of surfactant on surface tension

The surface tension of three systems was measured up to the CMC and presented in Figure 6.2

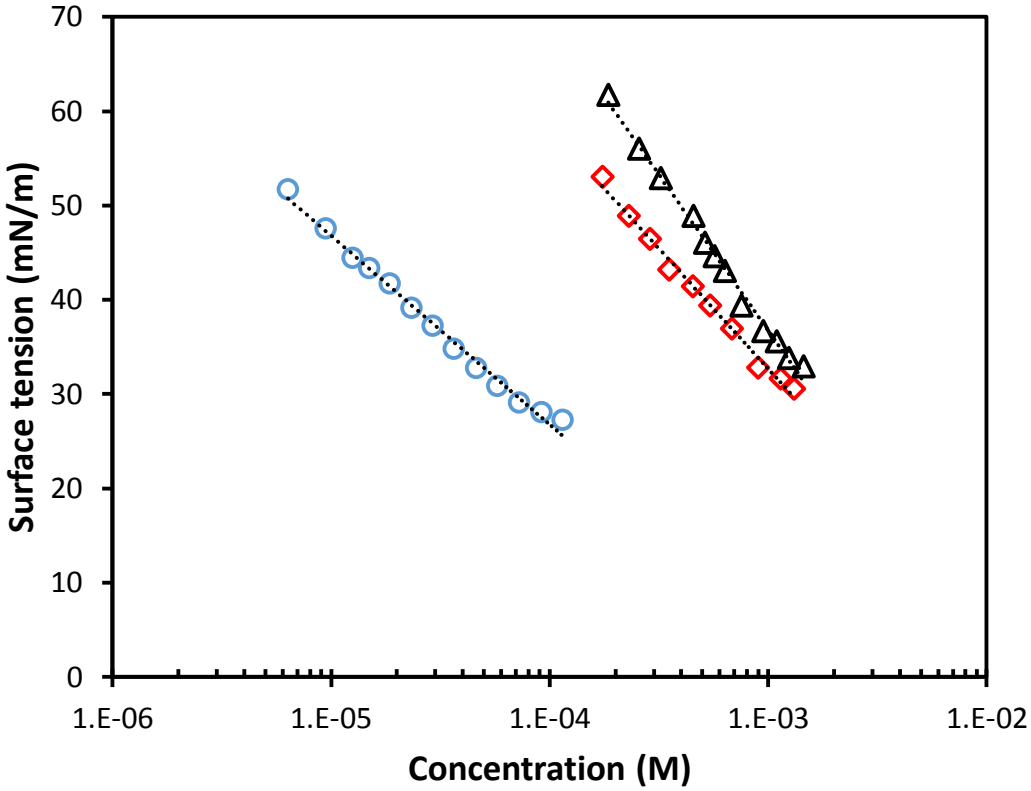

Figure 6.2. Equilibrium surface tension three Tritons up to the CMC

The Gibbs equation was employed and combined with these data to get Γ_s (as shown in Table 3.1) using the well-known procedure [128]. In order to maintain the saturated surface layer in the ball motion experiment, twice CMC was used for all systems. Hence, the surface tension at this concentration was used for temperature analysis.

Table 6.1. Adsorption and thermal-response of three surfactants

Surfactant	n_{EO}	Γ_s (mol/m^2)	A_2 (mN/m/K)	A_a (mm^2)	A_s (mm^2)	β (°)
X-100	9.5	3.60 x 10^{-6}	-0.24	0.217	1.733	65.6
X-405	35	4.59 x 10^{-6}	-0.274	0.259	1.674	60.6

X-705	55	5.95 x 10^{-6}	-0.302	0.448	1.297	35.1

Figure 6.3 showed the linear reduction of the surface tension for all solutions. In other words, A_2 is a positive constant for all surfactant solutions. The A_2 value of pure water is higher for all three Triton solutions.

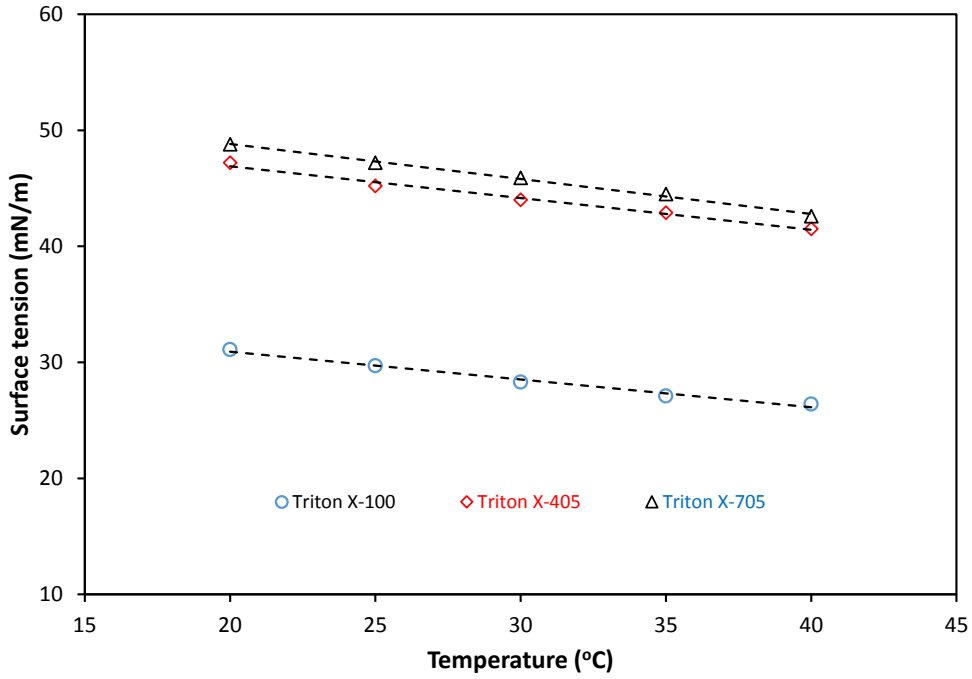

Figure 6.3. Impact of EO groups on surface tension behaviour: Surface tension as a function of temperature.

In Figure 6.4, A_2 is also linearly correlated to the product of Γ_s n_{EO}. The results validated Eq. (6-1).

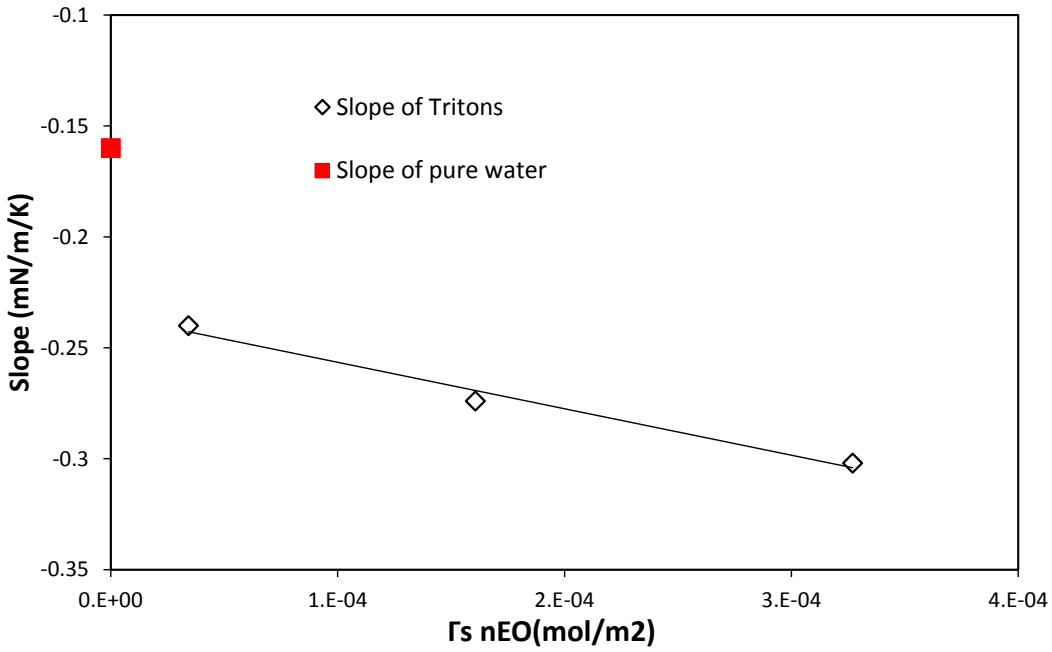

Figure 6.4. Gradient as a function of EO groups.

6.3.3. Influence of the surfactant on ball floating position

The surface tension and contact angle control the equilibrium position of the ball [117]. The ball is always floated for all systems in this study. However, the position changes as shown in Figure 6.5. The ball position is qualitatively higher with the increasing length of surfactant, which increased air/water surface tension (as shown Figure 6.3)

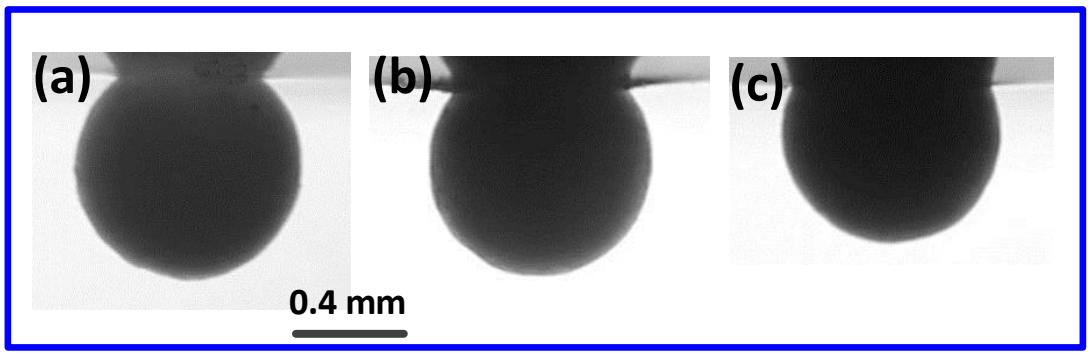

Figure 6.5. Cross-sectional images of the ball in (a) Triton X-100, (b) Triton X-405 and (c) Triton X-705.

The contact radius R_a (Figure 5.5) was determined manually from the images. The R_a was then used to calculate the contact angle and two contacting area (A_a and A_s) for each of the conditions. In literature, the value of θ_a for Teflon is well-reported as 108^o [117, 129, 130]. The value of ball position are included in and used as fixed parameters in the motion model.

6.3.4. Influence of the surfactant on ball movement

It should be noted that the ball did not move without adding salt in case of Triton X-405 and X-705. Figure 6.6 showed the position of ball movements on three surfactant solutions. It should be noted that the motion is slower with decreasing number of EO groups. However, the ball stopped as the shortest distance at the highest EO groups (Triton X-705). The previous numerical model was applied, using Euler's method with a step-size of 0.03s, to obtain E_{ff} and a_f (as shown in Table 6.2). The model fitted all three motions successfully. It can be seen that both driving and friction forces increased with increasing hydrophilicity. The values will be used to explore the molecular origin of the phenomena.

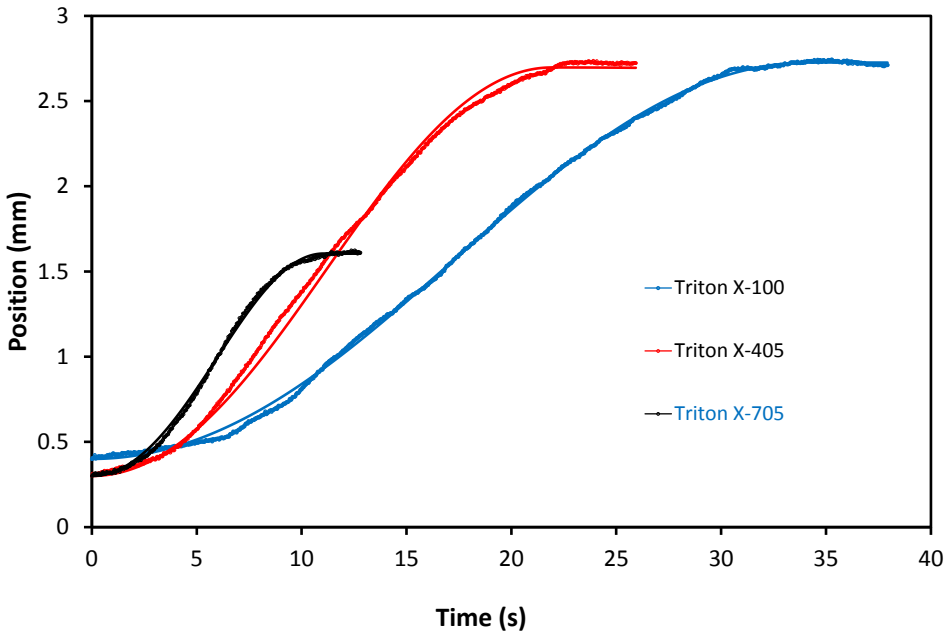

Figure 6.6. The position of ball movement on three Triton solutions.

Surfactant	E_{ff} (mN/m/K)	a_f (m/s^2)
X-100	9.81 x 10^{-8}	2.77 x 10^{-5}
X-405	2.43 x 10^{-7}	6.98 x 10^{-5}
X-705	1.03 x 10^{-6}	3.46 x 10^{-4}

Table 6.2. Impact of surfactant on modelling parameters.

To explore the molecular nature of the surfactant layer, the values of E_{ff} and a_f are evaluated against the molecular structure of the surfactant layer. From the model in chapter 5, we have:

$$E_{ff} = \frac{1}{m_a}\frac{C_T}{2\pi}A_a\cos(\beta)\frac{d\varepsilon}{dT}\Gamma_s n_{EO} \qquad (6\text{-}2)$$

As tabulated in , the contact area (A_a) and contact angle (β) changed with the surfactants. The other parameters (m_a, C_T and dε/dT) are independent on the surfactant. From Table 6.2, the correlation between $E_{ff}/A_a/\cos(\beta)$ and $\Gamma_s n_{EO}$ was obtained and plotted in Figure 6.7. The molecular basis of the phenomena has been validated by the strong linearity in Figure 6.7.

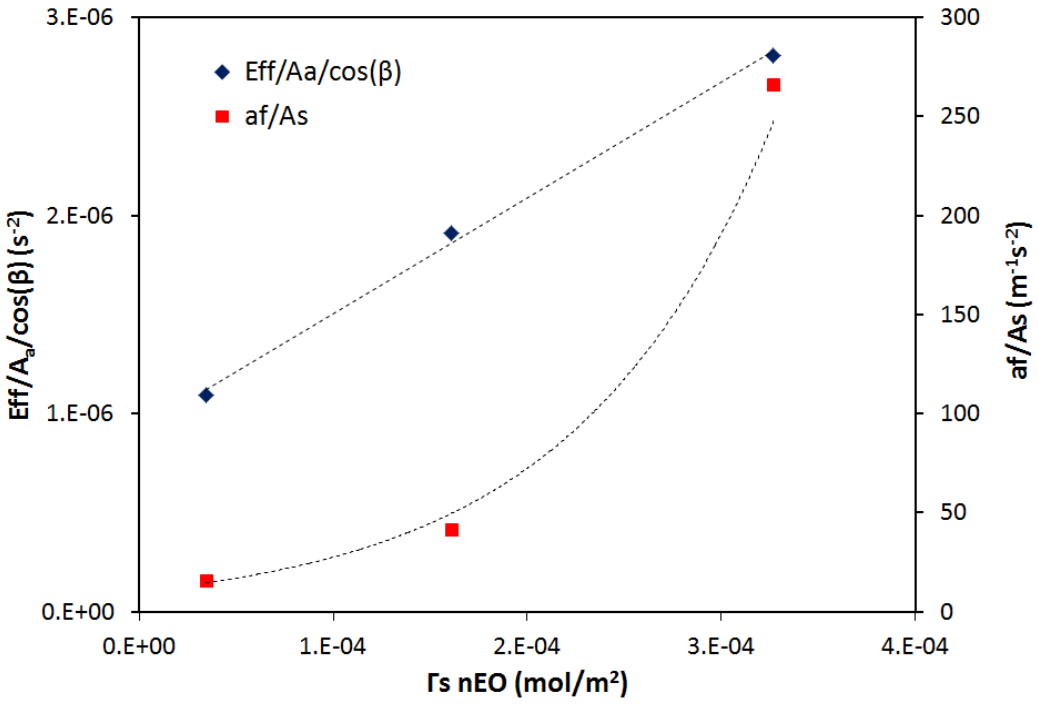

Figure 6.7. Correlations between driving/friction factors and number of EO.

In contrast, the contact area (A_s) and the friction coefficient between the ball and aqueous solution are used to determine the friction. The friction coefficient is correlated to the surfactant layer's viscosity which is dominated by the bonding of EO groups. It has been proved that the viscosity of poly EO solution was a non-linear function of number of EO groups [131]. Consequently, the viscosity and friction coefficient will be increased with the higher number of bonds. The viscosity-versus-

molecular length should obey a power law [132] as with common polymers. The data of a_f/A_s is consistent with a power relationship between bonds density and viscosity.

6.4. Summary

In this chapter, the thermal-driven surface movement was investigated with three Tritons, with increasing number of EO groups. It was found that the thermal gradient of surface tension is proportional to the number of EO, which indicated the dominance of EO groups. The EO groups correspondingly determined the movement, by controlling both driving and friction forces. The modelling on the driving force showed a linear correlation with number of EO groups. In contrast, the friction coefficient was increased, monotonically but non-linearly, with the number of EO groups on the surface layer. Both correlations are consistent with the thermal- and rheological-rules of EO bonding network. The results confirm the underpinning principles of thermal-surface flow. Furthermore, the new insights demonstrate possibilities to optimize the surface flow via changing surfactant structure.

Chapter 7 Conclusion and future recommendations

7.1. Thesis summary

Movement of either flow or object in multi-phase has been achieved enormous attention due to its large applications such as microfluidic industry. The driving forces for such motion can be varied from the modified-solid surface, thermal, chemicals, electricity and so on. On the other hand, the surface flow which is based on Marangoni effect has not been carefully quantified. In reality, it is hard to isolate the surface flow from the bulk flow. In this thesis, a general information of Marangoni effect and movement review has been carried out to understand the present trend of research.

It is well-known that surfactants have been used for many industrial applications due to their ability to decrease the surface tension of the solution at low concentration. Furthermore, surface tension is well-known for its sensitiveness with temperature. In this thesis, the surface tension of a series of Triton surfactants with increasing number of EO groups has been experimentally measured at different temperature with and without NaCl. The relationship has been found to be consistent with literature as the surface tension is a linear function of temperature. In addition, increasing hydrophilicity makes the slope of thermal gradient steeper. The presence of NaCl generally reduces the surface tension of surfactants, just like increasing temperature but there is no synergism between them.

The surface flow of the surfactant layer under thermal effect has been observed and quantified. The movement of surface flow was observed by using a floating Teflon ball. The source of thermal effect was produced by a Teflon-coated Tungsten wire connected to a power supply. The experiment was first carried out with the wire under the surface. This has led to the bulk flow occurring inside the solution. The wire was

then lifted up to the surface of the solution and the impact of bulk flow was eliminated. The change of temperature along the surface was small but enough to induce the movement of Teflon ball. A simplified model has been built to calculate the driving force of the motion.

The influence of hydrophilicity of the surfactants on such movement was also investigated. It has been found that increasing hydrophilic property led to the faster transportation but shorter distance. This would contribute one potential way to manipulate the surface flow in microfluidic applications.

In summary, we carried out experiment to observe the surface flow at the air/water interface under thermal effect. We also developed and verified theoretical models to understand the mechanism of the phenomena.

7.2. Future recommendations

- In this study, the quantified model has been proposed to model the movement of surface flow. One of the drawbacks of this model would be the simplification. It is necessary to develop a full model to understand clearer the nature of the phenomena. For example, molecular simulation of surfactant layer under thermal gradient can be applied.
- The observation of surface flow has been performed on different Triton surfactants. This research can be extended to other non-ionic surfactants to get insight the different factors which can influence the surface flow.
- The extension of this study can be obtained by applying different types of salt or hydroxides or acids on the surfactant solutions to make the change in surface tension.

- The phenomena cannot be observed in case of SDS and CTAB. It is interesting that the Teflon ball sunk once it was placed on the surface. The viscosity and density of surfactants should be taken into account to figure out their effect on the floating phenomenon. Future works should be developed to understand the molecular nature of this observation. Other surfactants will be taken into account such as polyoxyethylene alkyl ethers, or sugar and amino acid-based surfactants with a strong network of H-bonds to further understand this issue.
- The hydrophilic and lipophilic balance (HLB) value of each surfactants should be considered to further understand the effect of the number of EO and impurities on the surfactant flow.
- The CMC value of Triton X-405 and X-705 has not been fully explained as the surface tension increased after reach the minimum point. The future works will focus on the impurity of these surfactants to figure out the reason of such behaviour.
- One of the critical factors of controlling surface flow is time-dependent adsorption. This factor relies on the nature of surfactant such as structure, molecular weight, single or double tails, and polymeric or fluorinated surfactants. The future works will focus on these properties to further enhance the work in this thesis.

References

1. Brochard, F., Motions of droplets on solid surfaces induced by chemical or thermal gradients. Langmuir, 1989. **5**(2): p. 432-438.

2. Thiele, U., K. John, and M. Bär, Dynamical Model for Chemically Driven Running Droplets. Physical Review Letters, 2004. **93**(2): p. 027802.

3. Morgenthaler, S., C. Zink, and N.D. Spencer, Surface-chemical and -morphological gradients. Soft Matter, 2008. **4**(3): p. 419-434.

4. Ichimura, K., et al., Reversible change in alignment mode of nematic liquid crystals regulated photochemically by command surfaces modified with an azobenzene monolayer. Langmuir, 1988. **4**(5): p. 1214-1216.

5. Gallardo, B.S., et al., Electrochemical Principles for Active Control of Liquids on Submillimeter Scales. Science, 1999. **283**(5398): p. 57-60.

6. Rajagopalan, R., and P.C. Hiemenz, Principles of colloid and surface chemistry. Marcel Dekker, New-York, 3e édition, ISBN 0, 1997. **8247**(9397): p. 8.

7. Chang, C.-H. and E.I. Frances, Adsorption dynamics of surfactants at the air/water interface: a critical review of mathematical models, data, and mechanisms. Colloids and Surfaces A: Physicochemical and Engineering Aspects, 1995. **100**: p. 1-45.

8. Rhein, L.D., et al., Surfactants in personal care products and decorative cosmetics. Vol. 135. 2006: crc press.

9. ShamsiJazeyi, H., R. Verduzco, and G.J. Hirasaki, Reducing adsorption of anionic surfactant for enhanced oil recovery: Part I. Competitive adsorption mechanism. Colloids and Surfaces A: Physicochemical and Engineering Aspects, 2014. **453**: p. 162-167.

10. Rosen, M.J. and J.T. Kunjappu, Surfactants and interfacial phenomena. 2012: John Wiley & Sons.

11. Van Os, N.M., Nonionic surfactants: organic chemistry. Vol. 72. 1997: CRC Press.

12. Salager, J.-L., Surfactants types and uses. Firp Booklet, 2002(E300A).

13. Mucic, N., et al., Adsorption layer properties of alkyltrimethylammonium bromides at interfaces between water and different alkanes. Journal of colloid and interface science, 2013. **410**: p. 181-187.

14. Paria, S. and K.C. Khilar, A review on experimental studies of surfactant adsorption at the hydrophilic solid–water interface. Advances in colloid and interface science, 2004. **110**(3): p. 75-95.

15. Reichardt, C. and T. Welton, Solvents and solvent effects in organic chemistry. 2011: John Wiley & Sons.

16. Knoche, M., H. Tamura, and M.J. Bukovac, Performance and stability of the organosilicon surfactant L-77: effect of pH, concentration, and temperature. Journal of agricultural and food chemistry, 1991. **39**(1): p. 202-206.

17. Hinze, W.L. and E. Pramauro, A critical review of surfactant-mediated phase separations (cloud-point extractions): theory and applications. Critical Reviews in Analytical Chemistry, 1993. **24**(2): p. 133-177.

18. Zana, R., Aqueous surfactant-alcohol systems: a review. Advances in Colloid and Interface Science, 1995. **57**: p. 1-64.

19. Yang, Y., J. Dong, and X. Li, Micelle to vesicle transitions of N-dodecyl-1, ω-diaminoalkanes: Effects of pH, temperature and salt. Journal of colloid and interface science, 2012. **380**(1): p. 83-89.

20. Li, X., et al., Rich Self-Assembly Behavior from a Simple Amphiphile. ChemPhysChem, 2010. **11**(14): p. 3074-3077.

21. Fowler, C.I., et al., Emulsion polymerization of styrene and methyl methacrylate using cationic switchable surfactants. Macromolecules, 2011. **44**(8): p. 2501-2509.

22. Mihara, M., P. Jessop, and M. Cunningham, Redispersible polymer colloids using carbon dioxide as an external trigger. Macromolecules, 2011. **44**(10): p. 3688-3693.

23. Jasper, J.J., The surface tension of pure liquid compounds. Journal of physical and chemical reference data, 1972. **1**(4): p. 841-1010.

24. Vazquez, G., E. Alvarez, and J.M. Navaza, Surface tension of alcohol water+ water from 20 to 50. degree. C. Journal of chemical and engineering data, 1995. **40**(3): p. 611-614.

25. Adamson, A.W. and A.P. Gast, Physical chemistry of surfaces. 1967.

26. Miller, R., P. Joos, and V.B. Fainerman, Dynamic surface and interfacial tensions of surfactant and polymer solutions. Advances in Colloid and Interface Science, 1994. **49**: p. 249-302.

27. Phan, C.M., T.N. Le, and S.-i. Yusa, A new and consistent model for dynamic adsorption of CTAB at air/water interface. Colloids and Surfaces A: Physicochemical and Engineering Aspects, 2012. **406**: p. 24-30.

28. Eastoe, J. and J. Dalton, Dynamic surface tension and adsorption mechanisms of surfactants at the air–water interface. Advances in colloid and interface science, 2000. **85**(2): p. 103-144.

29. Prosser, A.J. and E.I. Franses, Adsorption and surface tension of ionic surfactants at the air–water interface: review and evaluation of equilibrium models.

Colloids and Surfaces A: Physicochemical and Engineering Aspects, 2001. **178**(1): p. 1-40.

30. Neys, B. and P. Joos, Equilibrium surface tensions and surface potentials of some fatty acids. Colloids and Surfaces A: Physicochemical and Engineering Aspects, 1998. **143**(2): p. 467-475.

31. Markin, V.S. and A.G. Volkov, Quantitative theory of surface tension and surface potential of aqueous solutions of electrolytes. The Journal of Physical Chemistry B, 2002. **106**(45): p. 11810-11817.

32. Wasan, D.T., M.E. Ginn, and D.O. Shah, Surfactants in chemical/process engineering. 1988: M. Dekker.

33. Gecol, H., et al., Use of surfactants to remove water based inks from plastic films. Colloids and Surfaces A: Physicochemical and Engineering Aspects, 2001. **189**(1): p. 55-64.

34. Kang, P.K. and D.O. Shah, Filtration of Nanoparticles with Dimethyldioctadecylammonium Bromide Treated Microporous Polypropylene Filters. Langmuir, 1997. **13**(6): p. 1820-1826.

35. Chiming, M. and Y. Xia, Mixed adsorption of sodium dodecyl sulfate and ethoxylated nonylphenols on carbon black and the stability of carbon black dispersions in mixed solutions of sodium dodecyl sulfate and ethoxylated nonylphenols. Colloids and Surfaces, 1992. **66**(3): p. 215-221.

36. Ma, C. and Y. Xia, Mixed adsorption of sodium dodecylsulfate and ethoxylated nonylphenol on TiO2 and the stability of TiO2 dispersions in sodium dodecylsulfate—ethoxylated nonylphenol mixed solutions. Colloids and Surfaces, 1992. **68**(3): p. 171-177.

37. Griffith, J.C. and A.E. Alexander, Equilibrium adsorption isotherms for wool/detergent systems: I. The adsorption of sodium dodecyl sulfate by wool. Journal of Colloid and Interface Science, 1967. **25**(3): p. 311-316.

38. Adamson, A. and A. Gast, Electrical aspects of surface chemistry. Physical chemistry of surfaces, 1997: p. 169.

39. Gao, Y., J. Du, and T. Gu, Hemimicelle formation of cationic surfactants at the silica gel–water interface. Journal of the Chemical Society, Faraday Transactions 1: Physical Chemistry in Condensed Phases, 1987. **83**(8): p. 2671-2679.

40. Brinck, J., B. Jönsson, and F. Tiberg, Kinetics of nonionic surfactant adsorption and desorption at the silica− water interface: One component. Langmuir, 1998. **14**(5): p. 1058-1071.

41. Tiberg, F., Physical characterization of non-ionic surfactant layers adsorbed at hydrophilic and hydrophobic solid surfaces by time-resolved ellipsometry. Journal of the Chemical Society, Faraday Transactions, 1996. **92**(4): p. 531-538.

42. Partyka, S., et al., The adsorption of non-ionic surfactants on a silica gel. Colloids and Surfaces, 1984. **12**(Supplement C): p. 255-270.

43. Nevskaia, D.M., A. Guerrero-Ruíz, and J. de D. López-González, Adsorption of Polyoxyethylenic Nonionic and Anionic Surfactants from Aqueous Solution: Effects Induced by the Addition of NaCl and CaCl2. Journal of Colloid and Interface Science, 1998. **205**(1): p. 97-105.

44. Zhu, B.-Y. and T. Gu, Surfactant adsorption at solid-liquid interfaces. Advances in Colloid and Interface Science, 1991. **37**(1): p. 1-32.

45. González-García, C.M., et al., Determination of the Free Energy of Adsorption on Carbon Blacks of a Nonionic Surfactant from Aqueous Solutions. Langmuir, 2000. **16**(8): p. 3950-3956.

46. Levitz, P., Aggregative adsorption of nonionic surfactants onto hydrophilic solid/water interface. Relation with bulk micellization. Langmuir, 1991. **7**(8): p. 1595-1608.

47. Brack, N., et al., Nonionic surfactants and the wool fibre surface. Colloids and Surfaces A: Physicochemical and Engineering Aspects, 1999. **146**(1): p. 405-415.

48. D Parfitt, G. and C. H Rochester, Adsorption from solution at the solid /liquid interface / edited by G. D. Parfitt and C. H. Rochester. 2017.

49. Giles, C.H., et al., 786. Studies in adsorption. Part XI. A system of classification of solution adsorption isotherms, and its use in diagnosis of adsorption mechanisms and in measurement of specific surface areas of solids. Journal of the Chemical Society (Resumed), 1960(0): p. 3973-3993.

50. Scriven, L. and C. Sternling, The marangoni effects. Nature, 1960. **187**(4733): p. 186-188.

51. Bénard, H., Les tourbillons cellulaires dans une nappe liquide. - Méthodes optiques d'observation et d'enregistrement. J. Phys. Theor. Appl., 1901. **10**(1): p. 254-266.

52. Rayleigh, L., LIX. On convection currents in a horizontal layer of fluid, when the higher temperature is on the under side. The London, Edinburgh, and Dublin Philosophical Magazine and Journal of Science, 1916. **32**(192): p. 529-546.

53. Block, M.J., Surface Tension as the Cause of Bénard Cells and Surface Deformation in a Liquid Film. Nature, 1956. **178**: p. 650.

54. Pearson, J.R.A., On convection cells induced by surface tension. Journal of Fluid Mechanics, 2006. **4**(5): p. 489-500.

55. Karbalaei, A., R. Kumar, and H.J. Cho, Thermocapillarity in microfluidics—a review. Micromachines, 2016. **7**(1): p. 13.

56. Oron, A., S.H. Davis, and S.G. Bankoff, Long-scale evolution of thin liquid films. Reviews of Modern Physics, 1997. **69**(3): p. 931-980.

57. Maki, K.L. and S. Kumar, Fast Evaporation of Spreading Droplets of Colloidal Suspensions. Langmuir, 2011. **27**(18): p. 11347-11363.

58. Tan, M.J., S.G. Bankoff, and S.H. Davis, Steady thermocapillary flows of thin liquid layers. I. Theory. Physics of Fluids A: Fluid Dynamics, 1990. **2**(3): p. 313-321.

59. Ostrach, S., Low-Gravity Fluid Flows. Annual Review of Fluid Mechanics, 1982. **14**(1): p. 313-345.

60. Davis, S.H., Thermocapillary Instabilities. Annual Review of Fluid Mechanics, 1987. **19**(1): p. 403-435.

61. Smith, M.K. and S.H. Davis, Instabilities of dynamic thermocapillary liquid layers. Part 1. Convective instabilities. Journal of Fluid Mechanics, 2006. **132**: p. 119-144.

62. Cazabat, A.M., et al., Fingering instability of thin spreading films driven by temperature gradients. Nature, 1990. **346**: p. 824.

63. Bowen, M. and B.S. Tilley, Thermally induced van der Waals rupture of thin viscous fluid sheets. Physics of Fluids, 2012. **24**(3): p. 032106.

64. Sáenz, P.J., et al., Stability and Two-phase Dynamics of Evaporating Marangoni-driven Flows in Laterally-heated Liquid Layers and Sessile Droplets. Procedia IUTAM, 2015. **15**(Supplement C): p. 116-123.

65. Sultan, E., A. Boudaoud, and M.B. Amar, Evaporation of a thin film: diffusion of the vapour and Marangoni instabilities. Journal of Fluid Mechanics, 2005. **543**: p. 183-202.

66. Kavehpour, P., B. Ovryn, and G.H. McKinley, Evaporatively-driven Marangoni instabilities of volatile liquid films spreading on thermally conductive

substrates. Colloids and Surfaces A: Physicochemical and Engineering Aspects, 2002. **206**(1): p. 409-423.

67. Deegan, R.D., et al., Contact line deposits in an evaporating drop. Physical Review E, 2000. **62**(1): p. 756-765.

68. Barash, L.Y., et al., Evaporation and fluid dynamics of a sessile drop of capillary size. Physical Review E, 2009. **79**(4): p. 046301.

69. Shih, A.T. and C.M. Megaridis, Thermocapillary flow effects on convective droplet evaporation. International journal of heat and mass transfer, 1996. **39**(2): p. 247-257.

70. Marek, R. and J. Straub, Analysis of the evaporation coefficient and the condensation coefficient of water. International Journal of Heat and Mass Transfer, 2001. **44**(1): p. 39-53.

71. Ajaev, V.S., Spreading of thin volatile liquid droplets on uniformly heated surfaces. Journal of Fluid Mechanics, 2005. **528**: p. 279-296.

72. Paxson, A.T. and K.K. Varanasi, Self-similarity of contact line depinning from textured surfaces. Nature Communications, 2013. **4**: p. 1492.

73. Checco, A., Liquid Spreading under Nanoscale Confinement. Physical Review Letters, 2009. **102**(10): p. 106103.

74. Checco, A., et al., Stability of Thin Wetting Films on Chemically Nanostructured Surfaces. Physical Review Letters, 2012. **109**(16): p. 166101.

75. Chaudhury, M.K. and G.M. Whitesides, How to Make Water Run Uphill. Science, 1992. **256**(5063): p. 1539-1541.

76. de Gennes, P.G., Wetting: statics and dynamics. Reviews of Modern Physics, 1985. **57**(3): p. 827-863.

77. Bonn, D., et al., Wetting and spreading. Reviews of Modern Physics, 2009. **81**(2): p. 739-805.

78. Snoeijer, J.H. and B. Andreotti, Moving Contact Lines: Scales, Regimes, and Dynamical Transitions. Annual Review of Fluid Mechanics, 2013. **45**(1): p. 269-292.

79. Ichimura, K., S.-K. Oh, and M. Nakagawa, Light-driven motion of liquids on a photoresponsive surface. Science, 2000. **288**(5471): p. 1624-1626.

80. Siewierski, L.M., et al., Photoresponsive Monolayers Containing In-Chain Azobenzene. Langmuir, 1996. **12**(24): p. 5838-5844.

81. Ueda, M., et al., Photocontrolled dispersibility of colloidal silica by surface adsorption of a calix[4]resorcinarene having azobenzene groups. Journal of Materials Chemistry, 1997. **7**(4): p. 641-645.

82. Ito, Y., et al., The Movement of a Water Droplet on a Gradient Surface Prepared by Photodegradation. Langmuir, 2007. **23**(4): p. 1845-1850.

83. Prins, M.W.J., W.J.J. Welters, and J.W. Weekamp, Fluid Control in Multichannel Structures by Electrocapillary Pressure. Science, 2001. **291**(5502): p. 277-280.

84. Dorri, N., P. Shahbazi, and A. Kiani, Self-Movement of Water Droplet at the Gradient Nanostructure of Cu Fabricated Using Bipolar Electrochemistry. Langmuir, 2014. **30**(5): p. 1376-1382.

85. Ban, T., et al., pH-Dependent Motion of Self-Propelled Droplets due to Marangoni Effect at Neutral pH. Langmuir, 2013. **29**(8): p. 2554-2561.

86. Banno, T., R. Kuroha, and T. Toyota, pH-Sensitive self-propelled motion of oil droplets in the presence of cationic surfactants containing hydrolyzable ester linkages. Langmuir, 2012. **28**(2): p. 1190-5.

87. Miura, S., et al., pH-induced motion control of self-propelled oil droplets using a hydrolyzable gemini cationic surfactant. Langmuir, 2014. **30**(27): p. 7977-85.

88. Phan, C.M., Rechargeable Aqueous Microdroplet. J Phys Chem Lett, 2014. **5**(8): p. 1463-6.

89. Čejková, J., et al., Dynamics of Chemotactic Droplets in Salt Concentration Gradients. Langmuir, 2014. **30**(40): p. 11937-11944.

90. Lagzi, I., et al., Maze Solving by Chemotactic Droplets. Journal of the American Chemical Society, 2010. **132**(4): p. 1198-1199.

91. Hanczyc, M.M., et al., Fatty Acid Chemistry at the Oil−Water Interface: Self-Propelled Oil Droplets. Journal of the American Chemical Society, 2007. **129**(30): p. 9386-9391.

92. Kim, H.S, et al. "Solutal Marangoni flows of miscible liquids drive transport without surface contamination." Nature Physics 13.11 (2017): 1105.

93. Graf, K. and M. Kappl, Physics and chemistry of interfaces. 2006: John Wiley & Sons.

94. Buzzacchi, M., P. Schmiedel, and W. von Rybinski, Dynamic surface tension of surfactant systems and its relation to foam formation and liquid film drainage on solid surfaces. Colloids and Surfaces A: Physicochemical and Engineering Aspects, 2006. **273**(1): p. 47-54.

95. Hunter, T.N., et al., Non-ionic surfactant interactions with hydrophobic nanoparticles: Impact on foam stability. Colloids and Surfaces A: Physicochemical and Engineering Aspects, 2009. **347**(1): p. 81-89.

96. Huang, C.-W. and C.-H. Chang, A laboratory study on foam-enhanced surfactant solution flooding in removing n-pentadecane from contaminated columns.

Colloids and Surfaces A: Physicochemical and Engineering Aspects, 2000. **173**(1): p. 171-179.

97. Pal, A., Photoinitiated gold sol generation in aqueous Triton X-100 and its analytical application for spectrophotometric determination of gold. Talanta, 1998. **46**(4): p. 583-587.

98. Tadros, T.F., Applied surfactants: principles and applications. 2006: John Wiley & Sons.

99. Inoue, T. and M. Monde, Enhancement of nucleate pool boiling heat transfer in ammonia/water mixtures with a surface-active agent. International Journal of Heat and Mass Transfer, 2012. **55**(13): p. 3395-3399.

100. Jeong, M., et al., Mass transfer performance enhancement by nanoemulsion absorbents during CO2 absorption process. International Journal of Heat and Mass Transfer, 2017. **108**(Part A): p. 680-690.

101. Nguyen, T.B. and C.M. Phan, Surface flow of surfactant layer on air/water interface. Colloids and Surfaces A: Physicochemical and Engineering Aspects, 2017. **530**(Supplement C): p. 72-75.

102. Cheng, L., D. Mewes, and A. Luke, Boiling phenomena with surfactants and polymeric additives: A state-of-the-art review. International Journal of Heat and Mass Transfer, 2007. **50**(13): p. 2744-2771.

103. Liu, R., J.-f. Liu, and G.-b. Jiang, Use of Triton X-114 as a weak capping agent for one-pot aqueous phase synthesis of ultrathin noble metal nanowires and a primary study of their electrocatalytic activity. Chemical Communications, 2010. **46**(37): p. 7010-7012.

104. Gittens, G., Variation of surface tension of water with temperature. Journal of Colloid and Interface Science, 1969. **30**(3): p. 406-412.

105. Cini, R. and M. Torrini, Temperature Dependence of the Magnetic Susceptibility of Water. The Journal of Chemical Physics, 1968. **49**(6): p. 2826-2830.

106. Kayser, W.V., Temperature dependence of the surface tension of water in contact with its saturated vapor. Journal of Colloid and Interface Science, 1976. **56**(3): p. 622-627.

107. Parmar, H., et al., Influence of microwaves on the water surface tension. Langmuir, 2014. **30**(33): p. 9875-9879.

108. Le, T.N., C.M. Phan, and H.M. Ang, Influence of hydrophobic tail on the adsorption of isomeric alcohols at air/water interface. Asia-Pacific Journal of Chemical Engineering, 2012. **7**(2): p. 250-255.

109. Fainerman, V.B., et al., Adsorption layer characteristics of Triton surfactants: 1. Surface tension and adsorption isotherms. Colloids and Surfaces A: Physicochemical and Engineering Aspects, 2009. **334**(1–3): p. 1-7.

110. Khan, A., A Liquid Water Model: Density Variation from Supercooled to Superheated States, Prediction of H-Bonds, and Temperature Limits. The Journal of Physical Chemistry B, 2000. **104**(47): p. 11268-11274.

111. Jorgensen, W.L. and J.D. Madura, Temperature and size dependence for Monte Carlo simulations of TIP4P water. Molecular Physics, 1985. **56**(6): p. 1381-1392.

112. Hyde, A., et al., Effects of microwave irradiation on the decane-water interface in the presence of Triton X-100. Colloids and Surfaces A: Physicochemical and Engineering Aspects, 2017. **524**: p. 178-184.

113. Phan, C.M., C.V. Nguyen, and T.T.T. Pham, Molecular Arrangement and Surface Tension of Alcohol Solutions. The Journal of Physical Chemistry B, 2016. **120**(16): p. 3914-3919.

114. Bau, H.H., Control of Marangoni–Bénard convection. International Journal of Heat and Mass Transfer, 1999. **42**(7): p. 1327-1341.

115. Islam, M.N. and T. Kato, Temperature Dependence of the Surface Phase Behavior and Micelle Formation of Some Nonionic Surfactants. The Journal of Physical Chemistry B, 2003. **107**(4): p. 965-971.

116. Nguyen, V.X. and K.J. Stebe, Patterning of small particles by a surfactant-enhanced Marangoni-Bénard instability. Physical Review Letters, 2002. **88**(16): p. 164501.

117. Extrand, C.W. and S.I. Moon, Using the Flotation of a Single Sphere to Measure and Model Capillary Forces. Langmuir, 2009. **25**(11): p. 6239-6244.

118. Cini, R., G. Loglio, and A. Ficalbi, Temperature dependence of the surface tension of water by the equilibrium ring method. Journal of Colloid and Interface Science, 1972. **41**(2): p. 287-297.

119. Israelachvili, J.N., Intermolecular and surface forces. 3rd ed. 2011: Academic press.

120. Potapov, A.V., M.L. Hunt, and C.S. Campbell, Liquid–solid flows using smoothed particle hydrodynamics and the discrete element method. Powder Technology, 2001. **116**(2–3): p. 204-213.

121. Lovass, P., et al., Maze solving using temperature-induced Marangoni flow. RSC Adv., 2015. **5**(60): p. 48563-48568.

122. Lach, S., S.M. Yoon, and B.A. Grzybowski, Tactic, reactive, and functional droplets outside of equilibrium. Chemical Society Reviews, 2016.

123. Wang, S. and C.N. Mulligan, Rhamnolipid Foam Enhanced Remediation of Cadmium and Nickel Contaminated Soil. Water, Air, and Soil Pollution, 2004. **157**(1): p. 315-330.

124. Tracton, A.A., Coatings technology handbook. 2005: CRC press.

125. Gittens, G.J., Variation of surface tension of water with temperature. Journal of Colloid and Interface Science, 1969. **30**(3): p. 406-412.

126. Du, Q., E. Freysz, and Y.R. Shen, Surface Vibrational Spectroscopic Studies of Hydrogen Bonding and Hydrophobicity. Science, 1994. **264**(5160): p. 826-828.

127. Kjellander, R. and E. Florin, Water structure and changes in thermal stability of the system poly(ethylene oxide)-water. Journal of the Chemical Society, Faraday Transactions 1: Physical Chemistry in Condensed Phases, 1981. **77**(9): p. 2053-2077.

128. Phan, C., et al., Surface Potential of Methyl Isobutyl Carbinol Adsorption Layer at the Air/Water Interface. The journal of physical chemistry. B, 2012. **116**(3): p. 980-986.

129. Wu, S., Surface tension of solids: An equation of state analysis. Journal of Colloid and Interface Science, 1979. **71**(3): p. 605-609.

130. Kamusewitz, H. and W. Possart, The static contact angle hysteresis obtained by different experiments for the system PTFE/water. International Journal of Adhesion and Adhesives, 1985. **5**(4): p. 211-215.

131. Ebagninin, K.W., A. Benchabane, and K. Bekkour, Rheological characterization of poly(ethylene oxide) solutions of different molecular weights. Journal of Colloid and Interface Science, 2009. **336**(1): p. 360-367.

132. Colby, R.H., L.J. Fetters, and W.W. Graessley, The melt viscosity-molecular weight relationship for linear polymers. Macromolecules, 1987. **20**(9): p. 2226-2237.

Appendix

Visual basic codes for tracing the position of Teflon ball

Dry friction model

```
Option Base 0

Option Explicit

Function velocity1 (t, yi, vi, Eff, Ho, af, n)

't next time, yi: initial y, vi: initial v, af: constant friction

Dim i, delt, y(1000), v(1000), dydt(1000), dvdt(1000), output(0, 4), theta, R

y(0) = yi: v(0) = vi: i = 1: delt = t / n

For i = 1 To n

R = (y(i - 1) ^ 2 + Ho ^ 2) ^ 0.5

'Debug.Print i, y(i - 1), v(i - 1), R, theta,

theta = Application.WorksheetFunction.Asin(y(i - 1) / R)

'Debug.Print i, y(i - 1), v(i - 1), R, theta, dydt(i), dvdt(i)

dydt(i) = v(i - 1): dvdt(i) = (BXm2 / R) * Cos(theta) - af

'Debug.Print i, v(i - 1), dydt(i), dvdt(i)

If i > 1 Then

If v(i - 1) < 0 Then

dvdt(i) = 0

End If
```

```
End If

'Debug.Print i, v(i - 1), dydt(i), dvdt(i)

y(i) = y(i - 1) + dydt(i) * delt

v(i) = v(i - 1) + dvdt(i) * delt

Next i

output(0, 0) = y(n)

output(0, 1) = v(n):

output(0, 2) = dydt(n - 1)

output(0, 3) = dvdt(n - 1)

velocity1 = output

End Function
```

Lubricated friction model

```
Function velocity2 (t, yi, vi, Eff, Ho, Cd, n)

't next time, yi: initial y, vi: initial v, Cd: drag

Dim i, delt, y(1000), v(1000), dydt(1000), dvdt(1000), output(0, 4), theta, R

y(0) = yi: v(0) = vi: i = 1: delt = t / n

For i = 1 To n

R = (y(i - 1) ^ 2 + Ho ^ 2) ^ 0.5

'Debug.Print i, y(i - 1), v(i - 1), R, theta,

theta = Application.WorksheetFunction.Asin(y(i - 1) / R)

Debug.Print i, y(i - 1), v(i - 1), R, theta, dydt(i), dvdt(i)

dydt(i) = v(i - 1): dvdt(i) = (BXm / R ^ 2) * Cos(theta) - Cd * v(i - 1)

'Debug.Print i, v(i - 1), dydt(i), dvdt(i)

If i > 1 Then

If v(i - 1) < 0 Then

dvdt(i) = 0

End If

End If

'Debug.Print i, v(i - 1), dydt(i), dvdt(i)

y(i) = y(i - 1) + dydt(i) * delt
```

```
v(i) = v(i - 1) + dvdt(i) * delt

Next i

output(0, 0) = y(n)

output(0, 1) = v(n):

output(0, 2) = dydt(n - 1)

output(0, 3) = dvdt(n - 1)

velocity2 = output

End Function
```

Attribution of authorship

1. Paper "***Surface flow of surfactant layer on air/water interface.*** Colloids and Surfaces A: Physicochemical and Engineering Aspects, **2017**. 530 (Supplement C): p. 72-75."

   Authors and full affiliations (Dr Chi M. Phan, Curtin University):

	Conception and design	Acquisition of data & method	Data conditioning & manipulation	Analysis & statistical method	Interpretation & discussion	Final approval
Dr Chi M. Phan	X			X	X	X
I acknowledge that these represent my contribution to the above research output. Signed.						

2. Paper "***Influence of surfactant hydrophilicity on the thermal-driven air/water surface flow***. ACS Omega, **2018**. 3 (8), 9060-9065.

   Authors and full affiliations (Dr Chi M. Phan, Curtin University):

	Conception and design	Acquisition of data & method	Data conditioning & manipulation	Analysis & statistical method	Interpretation & discussion	Final approval
Dr Chi M. Phan	X				X	X
I acknowledge that these represent my contribution to the above research output. Signed.						

3. Paper "***Influence of temperature on the surface tension of Triton surfactant solutions.*** The Journal of Surfactants and Detergents, **2018.** ***Accepted*** (DOI: 10.1002/jsde.12228)

   Authors and full affiliations (Dr Chi M. Phan, Curtin University):

	Conception and design	Acquisition of data & method	Data conditioning & manipulation	Analysis & statistical method	Interpretation & discussion	Final approval
Dr Chi M. Phan	X			X	X	X
I acknowledge that these represent my contribution to the above research output. Signed.						